NASA Technical Memorandum 105242
AIAA-91-3568

MPD Thruster Technology

Roger M. Myers
Sverdrup Technology, Inc.
Lewis Research Center Group
Brook Park, Ohio

Maris A. Mantenieks
National Aeronautics and Space Administration
Lewis Research Center
Cleveland, Ohio

and

Michael R. LaPointe
Sverdrup Technology, Inc.
Lewis Research Center Group
Brook Park, Ohio

Prepared for the
Conference on Advanced Space Exploration Initiative Technologies
cosponsored by AIAA, NASA, and OAI
Cleveland, Ohio, September 4-6, 1991

NASA

MPD Thruster Technology

Roger M. Myers
Sverdrup Technology, Inc.
NASA Lewis Research Center Group
Brook Park, OH 44142

Maris A. Mantenieks
NASA Lewis Research Center
Cleveland, OH 44135

Michael R. LaPointe
Sverdrup Technology, Inc.
NASA Lewis Research Center Group
Brook Park, OH 44142

Abstract

MPD thrusters have demonstrated between 2000 and 7000 seconds specific impulse at efficiencies approaching 40%, and have been operated continuously at power levels over 500 kW. These demonstrated capabilities, combined with the simplicity and robustness of the thruster, make them attractive candidates for application to both unmanned and manned orbit raising, lunar, and planetary missions. To date, however, only a limited number of thruster confiurations, propellants, and operating conditions have been studied. This work reviews the present status of MPD thruster research, including developments in the measured performance levels and electrode erosion rates, and theoretical studies of the thruster dynamics. Significant progress has been made in establishing empirical scaling laws, performance and lifetime limitations and in the development of numerical codes to simulate the flow field and electrode processes.

Introduction

Magnetoplasmadynamic (MPD) thrusters are currently being considered for applications as primary propulsion for both piloted and robotic and planetary missions. The high specific impulse provided by MPD thrusters, between 2000 and 7000 seconds, can reduce the spacecraft launch mass by more than a factor of two below that of chemical/aerobraked vehicles if the thruster systems operate with efficiencies over 50%. In addition, proper selection of mission scenario shows that the trip times can be made comparable to those achieved with high thrust systems (400 days to Mars) using reasonable extrapolations of current technology[1-3]. MPD thrusters have been tested in steady-state operation at power levels between 30 and 600 kW, and up to 20 MW in pulsed mode for diagnostic purposes. The potential simplicity and robustness of the MPD thruster may be a significant advantage over alternative electric propulsion technologies. This paper presents an overview of the current status of MPD thruster technology, including both experimental and theoretical research efforts.

Typical MPD thrusters, shown in Fig. 1a-c, consist of a central, thoriated tungsten cathode surrounded by an annular anode. The material used for the anode depends on whether it is actively or radiatively cooled. Propellant, usually argon or hydrogen, is injected into the rear of the chamber through an insulating wall. The propellant is heated, ionized, and accelerated by the current passing from anode to cathode and the Lorentz forces generated by the interaction of the current with either the self-induced or applied magnetic fields. The azimuthal self-induced magnetic field arises from the radial and axial distribution of the discharge current. An

external solenoid coil, typically placed outside the anode, is used to generate the axial and radial components of the applied magnetic field. The different electrode configurations, shown in Figure 1a - c reflect the diversity of the geometries studied: there are currently insufficient data to establish which thruster configurations will provide the required performance levels.

A considerable amount of MPD thruster research and technology development was performed in the 1960's and very early 1970's. Efforts were underway in government, industry and university laboratories to study both the self-induced and applied magnetic field devices. Between that time and 1988 most work focussed on purely self-field devices, and only in the last three years has there been renewed interest in applied-field thrusters. This renewal of interest in applied field thrusters arose primarily from the apparent inability of steady-state self-field devices to deliver the performance levels needed for propulsion applications. To date, the highest performance measured on a self-field thruster was obtained on a pulsed devise, which reached 5000 seconds specific impulse at 40% efficiency with 1.5 MW input power[4]. By contrast, the highest performance applied field MPD thruster produced 7000 seconds specific impulse at 70% efficiency when operated in a steady-state mode on lithium propellant with 30 kW input power[5]. For propellants other than lithium, both self and applied-field steady-state thruster performance has been limited to efficiencies below 40% and specific impulses below 3000 seconds. In general, applied field thrusters have produced higher performance than the purely self-field devices.

While the demonstrated performance levels indicate that MPD thrusters may be attractive for SEI class missions, a high power (200 kW - 1 MW), high performance, long life, MPD thruster has yet to be demonstrated. MPD thruster life is currently limited by cathode erosion. The longest test to date, conducted in 1969, lasted only 500 hrs at 30 kW[6]. Efforts today are focussed on isolating the power loss mechanisms, identifying the dominant applied-field thruster acceleration processes, and minimizing electrode erosion. Direct testing of 50 to 500 kW MPD thrusters for application to precursor missions[3] is underway, however, the stringent requirements on the test facility preclude immediate testing of a steady-state multimegawatt MPD thruster in current space simulation chambers[7,8]. These facilities can be modified to increase pumping speed as described in Ref. 7. The current facility limitations are forcing the development of scaling relationships and of experiments devoted to studying particular thruster phenomena, rather than a direct attack on high power thruster development.

Two major reviews of the MPD thruster research and technology efforts have been performed. The first, by Nerheim and Kelly[9], included both experimental and theoretical work conducted up to 1968. The second, by Sovey and Mantenieks[10], focussed on experimental measurements of thruster performance and life up to 1987, though it did not include an assessment of the status of theoretical models. Over the past four years considerable progress has been made in improving the performance of 100 - 200 kW steady-state thrusters by using applied magnetic fields, and in identifying the performance loss and life limiting mechanisms for MPD thrusters operated at powers between 30 kW and 10 MW. In addition to an expansion of the experimental efforts, significant improvements have occured also in the numerical codes used to study MPD thrusters. These models have grown from one dimensional, inviscid, single fluid codes to fully two dimensional (axisymmetric) two fluid codes including viscosity, finite rate ionizatio,n and wall heat transport. In addition, several efforts are underway to determine the impact of plasma microturbulence on the plasma transport coefficients.

The purpose of this report is to summarize the status of MPD thruster technology programs, including both experimental and theoretical components. The paper is divided into three sections, the first dealing with experimental measurements of thruster performance and power deposition, the second reviewing recent studies of MPD thruster cathode erosion, and the third presenting a summary of the ongoing theoretical work in the field.

MPD Thruster Performance

The performance of any electric thruster is governed by the thrust efficiency, η, and the specific impulse, I_{sp}, which are calculated from:

$$(a)\ \eta = \frac{T^2}{2\dot{m}VJ} \qquad (b)\ I_{sp} = \frac{T}{\dot{m}g_0} \tag{1}$$

where T is the thrust, $\dot{m}$ is the mass flow rate and V and J are the discharge voltage and current, repectively. Evaluating thruster performance therefore requires accurate measurements of thrust, propellant flow rate, and input power. By far the most challenging of these measurements is the thrust, which is subject to errors arising from the low thrust to weight ratio of the rocket, thermal and electromagnetic tares, and vacuum facility interactions. The recent work of Haag[11] illustrates the care that must be taken to ensure elimination of the thrust stand tares. Several previous efforts have addressed the impact of facility pressure on thruster performance[7-9]. Ambient pressure has been found to affect the thrust, terminal voltage, and electrode power deposition. These studies indicate that for open-throat thrusters (Fig. 1a) the test facility pressure during operation should be below 0.07 Pa, while for nozzle-type thrusters operating at high propellant flow rates this requirement can be relaxed to 1 Pa. In addition to thrust measurement errors, the actual mass flow rate in the thrust chamber may be significantly impacted by electrode erosion. This is particularly true for pulsed thrusters, in which the cathode mass loss may be 2-3 orders-of-magnitude higher than in a steady state thruster. In this work the data are reported as they appeared, no attempt was made to put them on a consistent basis with respect to potential sources of error.

The highest values of efficiency and specific impulse reported over the last four years are shown in Fig. 2. The data were separated according to propellant, whether the thruster was operated with an applied magnetic field, and whether the thruster was operated in quasi-steady or steady-state mode. The numbers next to the symbols refer to the appropriate references[8,21,22,26-30]. The power dissipated in the solenoid was not included in the performance calculations for applied-field thrusters. The highest performance reported, 40% efficiency at 3500 seconds specific impulse, was measured with a hydrogen propellant, quasi-steady, applied-field thruster. While no clear trends are evident, the only specific impulses over 2000 seconds were obtained using applied field thrusters. The performance measurements are replotted as a function of thruster power in Fig. 3 and 4. It appears from Fig. 3 that the efficiency does increase with input power, though there are substantial differences between the various thrusters tested. There is no such trend in the specific impulses shown in Fig. 4, as the highest value reported, 7000 seconds, was obtained using a steady-state applied-field thruster operated at 16 kW using hydrogen propellant. Note that the performance of the highest power steady-state thruster was rather low, reaching only 23% efficiency at 950 seconds specific impulse. This low value of specific impulse is most likely a result of the high mass flow rate used for the test. For the operating conditions used, the thruster was in a predominantly thermal acceleration regime.

While the applied-field MPD thrusters have demonstrated improved performance over self-field devices, little is known about their scaling characteristics. An empirical study where the anode and cathode radii and lengths were varied in a systematic fashion was recently performed to establish the required data base[8]. In that work, the anode and cathode radii were varied from 2.5 cm to 5.1 cm, and from 0.64 to 1.27 cm, respectively. The anode length was either 7.6 cm or 15.2 cm, and the cathode length was either 2.5 or 7.6 cm. A total of seven cylindrical geometries and one flared anode geometry were tested. The thrusters were all tested at an argon propellant flow tate of 0.1 g/s and a discharge current of 1000 A. The results of this study show that for a given mass flow rate and discharge current the thrust varies as

$$T \propto \frac{R_a^2}{k_1 L_c R_c} B + k_2 f(L_a) \tag{2}$$

and the voltage as

$$V \propto \frac{R_a^2}{k_3 R_c} B + k_4 f(L_a) \tag{3}$$

where R_a and R_c are the anode and cathode radii, the k's are constants, L_c is the cathode length, B is the magnetic field strength, and the second terms in these relationships simply reflect that while the anode length impacts both thrust and voltage, it does not affect the influence of the magnetic field. These results, and the data from which they were established, indicate that to increase the performance at a given applied-field strength, both electrodes should be short and that the anode to cathode radius ratio should be small. However, it appears that while decreasing the anode radius increased the magnitude of the efficiency over the operating range studied, this may not remain the case for applied-field strengths over 0.1T. This is due to an observed increase in the rate of efficiency rise with increasing applied-field strength as the anode radius was made larger. While the impact of the propellant flow rate and discharge current were not quantified, comparisons of hydrogen and argon propellants show a substantial benefit from using the lighter gas. Figure 5 shows a performance comparison for the two gases, obtained with a cylindrical thruster having a 2.5 cm radius, 7.6 cm length anode operated on 25 mg/s of each gas at a discharge current of 750A (Fig. 1a). Not only does hydrogen provide approximately 1000 sec. higher specific impulse at a given field strength, but also the discharge is stable over a broader operating range, yielding almost a factor of two increase in ultimate performance.

Performance Limiters

The performance of MPD thrusters is limited by several factors, including electrode power dissipation, frozen flow losses, and the so-called "onset" phenomenon. The term "onset" is currently used to describe a wide range of phenomena, including high frequency voltage fluctuations, anode spot formation, and enhanced erosion of the chamber[12,13]. Over the past four years several efforts have been devoted to detailed studies of all of these performance limiters.

The single largest power loss mechanism in MPD thrusters operated at power levels below 2-3 MW is anode power deposition[8,14-16]. The power deposited into the anode is given by

$$P_a = J \cdot \left(V_a + \frac{5}{2}\frac{kT_e}{e} + \Phi \right) + P_{conv} + P_{rad} \tag{4}$$

where the first three terms arise from current conduction into the anode, P_{conv} is a convective term due to the hot plasma flow, and P_{rad} accounts for radiation from the plasma. For low pressure devices (Fig. 1 a and c), the current conduction terms dominate, though for certain conditions P_{conv} and P_{rad} can reach 20% of the anode power[15]. For low power steady state thrusters up to 80% of the input power is deposited into the anode, leaving only 20% for plasma heating and acceleration. Several techniques for reducing the anode power fraction are currently under investigation, including injecting propellant near the anode surface and applying magnetic fields. The former technique increases the number of current carriers in the anode region and is thought to decrease V_A, while adding a magnetic field increases the total power deposited into the thruster and decreases the fraction of that power deposited into the anode. The latter effect is illustrated in Fig. 6, which shows calorimetric measurements of anode power deposition for a 2.5 cm radius, 7.6 cm length anode cylindrical thruster. The data show that increasing the applied-field strength from 0.01T to 0.15T decreased the anode power fraction from 80% to 60% for the thruster geometry shown in Fig 1a. However, the total anode power increased linearly with increasing field strength. These results show that the magnetic field increases power

deposited into the plasma more rapidly than it deposits power into the anode.

The cathode is not a significant power sink in steady-state thrusters, though its importance in quasi-steady thrusters, is poorly understood. Measurements made in steady-state thrusters show that the cathode consumes between 5% and 15% of the input power, depending on thruster geometry and operating condition[16,17]. No direct measurements exist for quasi-steady thrusters, though it appears that the cathode fall voltage (and thus cathode power deposition) is significantly higher for pulsed devices[18,19]. Terminal voltage measurements show a 20-40 V decrease when the thruster is operated steady-state as opposed to quasi-steady, with the most likely explanation being a decrease in cathode fall voltage[18]. This result not only indicates that power deposition measurements in quasi-steady thrusters may not apply to steady-state thrusters, but also implies that comparing theoretical voltage predictions with quasi-steady measurements may not be appropriate.

The other MPD thruster power loss mechanisms, listed in approximate order of importance, include propellant ionization, heat transferred to the rear chamber wall, unrecovered plasma thermal energy, exhaust divergence, plasma radiation and atomic excitation. There is substantial evidence for thrusters operated on argon propellant that the plasma is nearly fully ionized for most operating conditions, leading to an ionization power sink of 3.8×10^5 W/kg/s of flow rate. Ionization fractions for other propellants are not known. Preliminary estimates of heat transfer to the rear chamber wall show that the dominant heat source is the radiation from the cathode surface, which is limited by view-factor considerations to less than one-half the cathode power. Estimates of the unrecovered thermal energy vary widely due to the large uncertainty in the ion temperature, which may be between 5000 and 100,000 K[20].

The ultimate limit on MPD thruster performance is a consequence of the long thruster lifetimes required for the missions of interest. The thrusters must be operated under conditions where the electrode and insulator erosion rate is low and where the risk of catastrophic failure due to arc instabilities is minimized. It is apparent from several studies[4,12,20,22] that there are certain critical operating conditions, hereafter called "onset conditions", at which there is a rapid increase in the erosion rate and the appearence of localized, high current density arcs at the anode surface. The latter can lead to catastrophic failure of the thruster. For self-field thrusters both the onset condition and thruster performance are strongly correlated with the ratio $J^2/\dot{m}$, which fundamentally links the performance and life of these devices. It is interesting to note that several authors have found that using an applied magnetic field can extend the range of $J^2/\dot{m}$ over which a thruster can be operated[23,24]. In addition, applied-field thrusters may achieve the required performance levels at significantly lower discharge currents, permitting opration well below the critical values of $J^2/\dot{m}$. A detailed review of empirical studies of the onset condition for self-field thrusters condition was completed recently by Preble[13]. He established correlations between the value of $J^2/\dot{m}$ at which onset occurred and the electrode lengths, the interelectrode spacing, propellant injection site, and propellant flow rate for cylindrical thrusters operated using argon propellant. The critical $J^2/\dot{m}$ increased when the shorter electrode (either anode or cathode) length was increased, and decreased when the interelectrode spacing was increased. Injecting propellant near the anode generally increased the critical $J^2/\dot{m}$, though this trend also appeared to depend on the electrode geometry and magnitude of the propellant flow rate. Increasing the propellant flow rate decreased the critical $J^2/\dot{m}$ slightly. Preble was able to explain these correlations in a preliminary fashion by invoking an electrothermal instability, the threshold of which was reached when the propellant was fully ionized.

Other experimental studies of the onset condition have focussed on plasma microturbulence. Researchers at Princeton University have experimentally measured the plasma dispersion relation and quantified the frequency dependence of density and temperature fluctuations in both 9 kW steady-state thruster and a 2-10 MW quasi-steady thruster[20,25]. For both these devices, spanning three orders-of-magnitude in power level, they found that most unstable mode of plasma microturbolence was the lower hybrid drift instability. It is clear that the instability may have a dramatic and sudden effect on plasma transport properties, although the connection between the instability and thruster performance limits has not been quantified.

MPD Thruster Lifetime

Cathode erosion has been identified as the major life limiter of MPD thrusters. First order calculations of propulsion requirements for lunar and Mars cargo vehicles indicate that the total impulse and life per thruster should be between $1x10^8$ to $1x10^9$ N-s and 2000 - 8000 hrs, respectively. These estimates assumed a specific impulse of 2000-5000 s and a power range per thruster between 0.5 and 3 MW. The lowest, most reliable cathode erosion rates measured prior to 1987 yielded predicted total impulse values that were two to three orders-of-magnitude below the estimated requirements defined above[10]. Such estimates, however, were difficult to make because the reported erosion rates varied over five orders-of-magnitude. Within the last few years significant progress has been made in both the measurement of erosion rates, cathode surface diagnostics, and in the theoretical understanding of MPD thruster cathode erosion processes.

The most recent measurements of steady-state and quasi-steady thrusters are listed in Table I, where the erosion rates are listed as mass lost per unit charge transferred through the cathode surface. The mass loss rates range from $5x10^{-4}$ to 0.2 μg/C for steady-state thrusters and 0.2 to 60 μg/C for quasi-steady thrusters. Clearly quasi-steady thrusters have much higher cathode erosion rates than steady-state thrusters, though there is some overlap for quasi-steady thrusters operated with low work function, barium impregnated, cathodes. The lowest values of steady-state thrusters were obtained at the University of Stuttgart using a nozzle-type thruster operating with high purity propellant.

The large differences between quasi-steady and steady-state erosion rates are readily explained by considering the electron emission mechanisms for the two operating modes. For quasi-steady thrusters, electron emission from a cold cathode is achieved by field enhanced thermal emission. The current attaches the cathode via highly mobile arc spots, typically between 10 and 50 μm in diameter[31,36,38], characterized by high current density ($> 10^{11}$ A/cm^2) and high local temperature ($>$ 5000 K). This emission mode is characterized by tungsten droplet ejection and strong evaporation, which is manifested by small "craters" from several microns to a tenth of a millimeter in size[31]. The cold cathode erosion rate of quasi-steady thrusters depends on the pulse frequency, pulse duration and the power applied. The use of an applied magnetic field reduced the cathode erosion rates by approximately a factor of two in two of the tests reported in Table 1[23,29].

Several investigators have varied the duration of steady-state tests to permit separation of the erosion rates characterizing the ignition and steady-state phases of operation. The ignition mode erosion rate generally varies from 5-30 μg/C[17,18,33,39], values which are close to those measured for quasi-steady thrusters operated with the same cathode material. The lowest erosion rate during the ignition mode was measured during single "shot" measurements. Higher erosion rates were measured during multiple "shot" runs, with the erosion rate decreasing with increasing number of "shots" during a test[33]. The type of propellant did not effect the ignition mode erosion rate[33]. For steady-state MPD thruster operation lasting many hundreds of hours the ignition rate should not significantly contribute to the total erosion rate of the cathode.

The steady-state thermal emission mode is reached when the cathode reaches a sufficiently high bulk temperature to permit electron emission in a diffuse mode of current attachment. Surface temperature measurements made using imaging techniques[17] show that thermionic emission governed by the Richardson equation appears to explain electron emission from the cathode[17,33,35]. This transition from ignition mode to steady state diffuse mode has been observed using high speed photography[17]. During the steady-state mode the surface temperature of the cathode can be substantially below 3200 K with current densities between 10 - 100 A/cm^2.

The relatively large differences in the steady-state erosion rates listed in Table 1 can be explained by considering the erosion mechanisms and the different thruster geometries used for the tests. Simultaneous measurements of cathode erosion rates and surface temperature distributions show that evaporation plays a

dominant role in the cathode mass loss. Estimates show that sputtering erosion does not contribute significantly for typical cathode temperatures and ion energies. While the maximum erosion rate appears to be determined by the vacuum evaporation rate of the cathode material, the actual net mass loss rate can be dramatically reduced by backscattering of the evaporated atoms off ambient gas atoms which return the material to the cathode surface. In addition, ionizing collisions between evaporated atoms and electrons yield ions which are pulled back to the cathode by the electric field. The influence of these processes on the cathode mass loss rate can be estimated by evaluating the appropriate mean-free paths as suggested by Myers[17], or by considering the ambient vapor pressure as suggested by Polk[35]. The hypothesis that the erosion rate of a cathode is governed by the backscattering mechanisms was confirmed at Stuttgart[33] and in the Soviet Union[37]. As shown in Fig. 7 for a benchtop arc experiment, the erosion rate was found to decrease with increasing ambient pressure. Indirect evidence of this phenomena is the constant erosion rate measured as a function of discharge current by Schrade[31] at low discharge current levels (2-4 KA) and the relatively large variation of cathode erosion rates measured as a function of discharge current by Polk[36]. It is clear that the influence of ambient pressures on backscattering rates fundamentally couple the thruster life, the thruster geometry, and the operating conditions.

For the nozzle-type thrusters operated at the University of Stuttgart, the ambient pressures sorrounding the cathode lead to high backscatting rates. In this case, the net loss due to evaporation is reduced, and other mass loss mechanisms play a larger role. This may explain the impact of propellant purity found at the University of Stuttgart, which indicates that surface oxidation plays a significant role[18,33,35]. These tests, conducted with hydrogen, argon, and nitrogen, clearly showed that eliminating water and oxygen from the propellant using a chemical filter reduced the cathode erosion rate by up to a factor of twenty. This is the first time this effect has been reported for MPD thrusters.

The importance of the cathode material arises due to its influence on the surface work function, which is the energy required to liberate an electron from the metal. A small reduction in work function can lead to a large drop in the cathode surface temperature required to emit a given current density. This, is turn, can lead to a large drop in the material evaporation rate as it is exponentially dependent on temperature. For this reason most cathodes utilize a small amount of low work function impregnant material, usually 2% thorium oxide. Experiments have clearly shown the importance of having the low work function material[33]. However, for the thoriated tungsten the evaporation rate of the thorium from the surface exceeds the diffusion rate to the surface when the cathode temperature exceeds 1800 to 2300 K[17,35]. Since the surface temperature of a 2% thoriated tungsten cathode in an MPD thruster usually exceeds these limits, the net loss of the low work function material will result in a relatively quick failure of the cathode, unless backscattering limits the escape of low work function material. Experiments using both new and slightly used ($\sim$2 hrs) cathodes indicated a small ThO_2 loss during the first several hours of operation[33,35]. Several hours of operation after the "conditioning" of the cathode indicated no more ThO_2 loss as inferred from a constant tip temperature during the test[35]. Some recent tests have explored using barium oxide impregnated cathodes in steady-state thrusters[32] though the results were inconclusive.

The discussion of the erosion mechanisms and the results of recent erosion rate measurements of an MPD cathode operating in a steady-state diffuse mode leads to the following conclusions: 1) Evaporation appears to be the dominant erosion mechanism of MPD thruster cathodes, 2) The ambient pressure at the cathode surface can substantially affect the erosion rate of the cathode, 3) the impact of propellant purity appears to be substantial for thrusters operated at relatively high pressure, 4) the loss of low work function material impacts the cathode lifetime via its influence on the surface temperature. These factors indicate that the simple loss parameter of mass loss per unit charge is not adequate to evaluate erosion rates of MPD thruster cathodes.

MPD Thruster Models

As discussed in the previous sections, MPD thrusters have undergone extensive experimental development since the early 1960's. In contrast, a detailed theoretical understanding of MPD thruster operation

has been slowed by the complex nature of the coupled electromagnetic and gasdynamic acceleration processes. Simplified analytical and numerical simulations using 1D and quasi-1D approximations of the fluid magnetohydrodynamic equations have provided valuable insights into both self-field and applied-field MPD thruster operation, but they are constrained in their ability to predict detailed thruster performance. The removal of such limitations via 2D and quasi-2D modeling has recently become practical with the emergence of high-speed computational facilities, allowing model validation and refinement using the existing experimental data base, while in return establishing a theoretical basis to guide further experimentation.

Governing Equations

The equations used to model MPD thruster dymamics are generally based on the fluid magnetohydrodynamic (MHD) equations, which are valid in the collisional plasma regimes of interest for MPD thruster operation[40]. The full set of equations includes coupled electromagnetic field and plasma flow equations, which together with expressions for the equation of state, electromagnetic and thermal transport coefficients, and ionization/recombination processes provide a complete description of the system. A fundamental exposition of the MHD formulation is provided by Sutton and Sherman[41], the salient features of which are reproduced below.

Electromagnetic Field Equations.

The basic set of electromagnetic equations includes the full complement of Maxwell's equations:

$$\begin{aligned} (a)\ \nabla\cdot\vec{B} &= 0 \qquad & (b)\ \nabla\times\vec{B} &= \mu_0\vec{j} \\ (c)\ \nabla\cdot\vec{E} &= \rho_e/\epsilon_0 \approx 0 \qquad & (d)\ \nabla\times\vec{E} &= -\frac{\partial\vec{B}}{\partial t} \end{aligned} \tag{5}$$

where $\vec{E}$ and $\vec{B}$ are the vector electric and magnetic fields, respectively, and $\vec{j}$ is the electric current density. The current density is related to the electromagnetic fields and plasma flow properties through a generalized Ohm's law, usually given in the form:

$$\vec{j} = \sigma\left[\vec{E} + \left(\vec{v}\times\vec{B}\right)\right] - \frac{\Omega}{B}\left(\vec{j}\times\vec{B}\right) + (1-\alpha)^2\frac{\Omega\Omega_i}{B^2}\left[\left(\vec{j}\times\vec{B}\right)\times\vec{B}\right] \tag{6}$$

The quantity σ is the electrical conductivity, $\vec{v}$ is the plasma flow velocity, and α is the ionization fraction of the plasma. Ω is the electron Hall parameter, which is the product of the electron cyclotron frequency and the electron collision time, while Ω_i is an equivalent expression for the ion Hall parameter, defined in terms of the ion cyclotron frequency and ion-neutral collision time. The ion Hall parameter enters into the ion slip term, which allows for incomplete coupling between the ions and neutral gas particles in a partially ionized plasma.

The electric field distribution may be obtained by rearranging Ohm's law:

$$\vec{E} = -\nabla\phi = \frac{1}{\sigma}\left[\vec{j} + \frac{\Omega}{B}\left(\vec{j}\times\vec{B}\right)\right] - \left(\vec{v}\times\vec{B}\right) \tag{7}$$

where ϕ is the electric potential. The radial component of the electric field may then be integrated from cathode to anode to determine the potential drop across the plasma.

A magnetic transport equation may be derived by combining Maxwell's equations with the generalized Ohm's law:

$$\begin{aligned} \nabla \times \vec{E} &= -\frac{\partial \vec{B}}{\partial t} \\ &= \nabla \times \left(\frac{\nabla \times \vec{B}}{\mu_0 \sigma} \right) + \nabla \times \left[\frac{\Omega}{\mu_0 \sigma B} \left((\nabla \times \vec{B}) \times \vec{B} \right) \right] - \nabla \times \left(\vec{v} \times \vec{B} \right) \end{aligned} \tag{8}$$

Solving the azimuthal component of the above equation provides the induced azimuthal magnetic field distribution. The azimuthal magnetic field is a function of the total discharge current J, hence a streamfunction $\psi \equiv rB_\theta \sim r(J/r) \sim J$ may be used to represent lines of total enclosed current.

The radial and axial current densities may be obtained from the calculated self-magnetic field distributions:

$$\begin{aligned} j_r &= -\frac{1}{\mu_0} \frac{\partial B_\theta}{\partial z} \\ j_z &= \frac{1}{\mu_0} \left(\frac{1}{r} \frac{\partial}{\partial r} (r B_\theta) \right) \end{aligned} \tag{9}$$

The azimuthal current density j_θ, which is due to the applied magnetic field, may be obtained from the azimuthal component of the general Ohm's law. The applied magnetic field components may be specified *a priori* or obtained from the solution of Maxwell's equations for an external current distribution.

Fluid Equations

The fluid equations encompass the conservation equations of mass, momentum, and energy, coupled with thermodynamic and caloric equations of state, ionization and recombination processes, chemical kinetics if the flow is reacting, and expressions for the plasma transport coefficients.

The conservation of mass for a compressible fluid is given by:

$$\frac{\partial \rho}{\partial t} + \nabla \cdot (\rho \vec{v}) = 0 \tag{10}$$

where ρ is the plasma mass density. Excluding ambient gas entrainment or electrode erosion, the mass conservation law states that the amount of propellant mass injected into the thruster per unit time must equal the amount of mass exhausted from the thruster per unit time.

The conservation of momentum yields an equation of motion for the plasma, given by:

$$\rho \left(\frac{Dv}{Dt} \right) = -\nabla p + \left(\vec{j} \times \vec{B} \right) + \overline{\Psi} \tag{11}$$

where p is the plasma pressure, $\overline{\Psi}$ is the viscous body force, and D/Dt denotes the advective derivative:

$$\frac{D}{Dt} \equiv \frac{\partial}{\partial t} + (\vec{v} \cdot \nabla) \tag{12}$$

For a self-field thruster, the components of the electromagnetic $\overline{j} \times \overline{B}$ body force simplify into an axial ($j_r B_\theta$) body force, which provides direct electromagnetic thrust ("blowing"), and a radial ($-j_z B_\theta$) body force, which provides electromagnetic compression of the plasma and a subsequent pressure force along the cathode surface ("pumping"). The electromagnetic body forces become significantly more complex for an applied-field thruster, where the interaction of the discharge current with the applied magnetic fields give rise to azimuthal body forces. The azimuthal body force can impart rotational motion to the plasma, which might be partially recovered as thermal energy (leading to enhanced electrothermal thrust) or converted to directed thrust via interactions with the applied magnetic field. Additional radial and axial body forces may be generated through interactions between the induced azimuthal current density and the applied magnetic field components. Viscous body forces and unbalanced pressure gradient forces must also be incorporated into a complete description of the plasma flow. While experimentally robust, the MPD thruster operates via some rather complex acceleration mechanisms.

A general form for the conservation of energy, which expresses a balance between the energy sources and sinks in the plasma, is given by:

$$\rho \frac{Dh}{Dt} = \frac{Dp}{Dt} + (\vec{E} + \vec{v} \times \vec{B}) \cdot \vec{j} - \nabla \cdot \vec{q} + \Phi_V \qquad (13)$$

The quantity h is the specific enthalpy, where the second term on the right is the Joule heating term, Φ_V is the viscous dissipation function, and $\overline{q}$ is the heat-flux vector. For models incorporating more than one fluid species (e.g. ions, electrons, and/or neutrals treated separately), individual conservation equations for each species must be used. The species momentum and temperature equations are then coupled through collision integrals to allow interactions between each plasma component. Ionization and recombination processes may be used to evaluate the ion, electron, and neutral species number densities, in concert with a quasi-neutrality approximation such that the calculated ion and electron number densities are equivalent.

The fluid equations are closed with a thermodynamic equation of state relating the plasma pressure, density, and temperature, a caloric equation of state relating the specific enthalpy to the plasma density and temperature, and expressions for the plasma transport coefficients (viscosity, thermal conductivity, and electrical conductivity).

Approximations

The full set of coupled, nonlinear partial differential equations used to model the MPD thruster plasma interactions present a formidable challenge for current numerical simulation techniques. Consequently, authors have employed simplifying assumptions to make the system dynamics more tractable. Table 2 lists the approximations used in several recent MPD thruster models[42-63], defined according to the assumed plasma properties and model geometries. The utility of the various approximations, and their validity for modeling the MPD thruster, are discussed below.

Plasma Species

The fluid approximations outlined above are valid for a collisional plasma, in which the electrons and ions separately relax to local thermodynamic equilibria over time scales which are short compared with changes in the overall plasma conditions, and in regions small compared with the overall plasma dimensions. The most simple fluid approximation is to ignore differences in the electron and ion species, and assume the plasma consists of a single conducting fluid which is described by a single mass density and a single (bulk) fluid velocity. This one-fluid approach leads to some ambiguity in definitions of the plasma transport coefficients, which are usually defined in terms of the separate electron and ion transport properties[41]. In addition, such effects as ambipolar diffusion, electrode sheath formation, ionization processes, and plasma instabilities cannot

be directly modeled with a single fluid approximation. Using a multi-species model (separate ion and electron species, and possibly an additional neutral species) circumvents these limitations, and provides a more accurate treatment of the transport phenomena; however, additional accuracy is obtained at the cost of increased complexity in solving separate density, momentum, and energy equations together with the associated species momentum and energy coupling models. Due to this added complexity, the one-fluid approach has been used extensively in MPD thruster modeling, and has provided a somewhat crude but effective method to gain insight into the general plasma behavior under a variety of operating conditions.

Plasma Temperature

Several of the models listed in Table 2 have employed a single temperature approximation in conjunction with a single fluid assumption to simplify the governing equations. While providing a useful first estimate of the plasma dynamics, the single temperature approximation may lead to gross inaccuracies in the plasma transport coefficients, which are sensitive to the plasma electron and ion temperatures[41]. Models which incorporate separate species energy equations (Table 2) have predicted significantly different electron and heavy particle temperatures. Such results indicate the plasma may not be in thermal equilibrium in many operating regimes of interest, and illustrate the disparity between single fluid models and the real plasmas which they model. Although the complexity of a multi-species, multi-temperature plasma model may not be warranted in the initial stages of model development, it is clear that separate electron and ion temperatures should be incorporated to provide more accurate predictions of the plasma transport coefficients.

Plasma Ionization

The assumption that the plasma is fully, singly ionized has been incorporated into most single fluid and multi-species MPD thruster models, despite the varying degrees of ionization observed experimentally[16,64]. This assumption does not significantly affect the classical plasma transport coefficients due to their weak logarithmic dependence upon the plasma number density. However, the transport coefficients are sensitive to the plasma species collision times, which in turn are inversely proportional to the plasma species number desities. Consequently, an accurate calculation of the plasma ionization fraction is required for an accurate evaluation of the Hall terms appearing in the generalized Ohm's law. In addition, a knowledge of the ionization state of the plasma is important for accurately modeling electrode sheaths[65,66], boundary layer flows[67], and plasma instabilities [13,20,68-75], which are not generally included in MPD thruster flow models due to the added complexity they bring to the problem. Discussions of nonequilibrium plasma ionization processes in self-field MPD thrusters may be found in references 76-80.

Miscellaneous Plasma Properties.

Hall Effect.

In the absence of a magnetic field, conduction electrons will follow electric field lines between the cathode and anode. In the presence of either induced or applied magnetic fields, these simple electron trajectories become curved[41], giving rise to a transverse current ("Hall" current) in a direction orthogonal to both the electric and magnetic fields. The magnitude of the transverse Hall parameter (Ω) depends upon the ratio of the electron cyclotron frequency to the electron collision frequency. The Hall current becomes important when $\Omega \approx 1$, and dominates the system dynamics when $\Omega >> 1$. The Hall effect skews the current distributions between the electrodes, causing current to concentrate upstream along the cathode and downstream along the anode (Fig. 8).

Viscosity.

Viscous effects cause a dissipation of directed kinetic energy into thermal energy with a consequent reduction of thrust efficiency. Viscous dissipation may significantly contribute to heating the heavy plasma

species, driving the ion temperature to equal, and in some instances exceed, the electron temperature[56,80,81].

Ion Slip.

All single fluid and most multi-species models assume the ion motion is equivalent to the bulk plasma motion. In operating regimes characterized by low plasma densities and high magnetic field strengths, however, the collisions between plasma ions and neutral particles may be insufficient to keep the ion motion coupled to the neutral gas flow. The ions may then cross the interelectrode gap or proceed on their own trajectories without contributing to the bulk fluid acceleration, causing a decrease in thrust efficiency. In single fluid models, and in models which assume a fully ionized plasma, the ion motion is identical with the bulk plasma motion, and the ion slip term is zero by definition.

Status of MPD Thruster Modeling

In their review paper, Nerheim and Kelley[9] provided an account of the general status of MPD thruster theory as of 1967. Relevant sections of their review article are summarized below, to provide a benchmark against which more recent MPD thruster modeling efforts may be compared.

The electromagnetic force produced by the interaction of an applied current and self-induced magnetic field had been derived analytically by Maecker[82] in 1955, and incorporated to explain self-field MPD thruster acceleration processes by the mid- 1960's. The electromagnetic force, in the absence of an applied magnetic field, has the form:

$$F_s = \frac{\mu_0 J^2}{4\pi}\left(\ln\frac{r_a}{r_c} + C\right) \tag{14}$$

where F_s is the self-induced electromagnetic force (thrust), J is the total discharge current, r_a and r_c are the anode and cathode radii, respectively, and C is a constant, which ranges in value from 0.25 if the current distribution is uniform over the cathode surface (excluding the cathode tip), to 0.75 if the current is uniformly distributed over the cathode tip[83]. This expression is popularly known as the "bJ^2 law", where b incorporates the various constants into a single thrust coefficient. The bJ^2 law works surprisingly well to predict self-field thrust when the thruster geometry is sufficiently simple (such that r_a and r_c are well defined) and electrothermal thrust contributions can be ignored. The simple derivation fails for thruster geometries more complex than cylindrical electrodes, and for thruster operating regimes where the thrust is produced primarily by thermal expansion of the propellant rather than electromagnetic acceleration.

Although thrust-producing mechanisms have been postulated for applied-field MPD thrusters, no comparable analytic expression relating electromagnetic thrust to engine operating parameters has yet been derived. One such mechanism discussed in Nerheim and Kelley (and the references therein) invokes the electromagnetic interaction between the applied current and the applied magnetic field to create an azimuthal torque on the plasma, which imparts rotational kinetic energy to the ionized propellant. The rotational energy might then be converted to directed kinetic energy through expansion in a magnetic nozzle[84,85], since the angular velocity must decrease to conserve angular momentum as the plasma expands, and the decrease in angular velocity must be accompanied by an increase in axial velocity to conserve kinetic energy. A second applied field acceleration mechanism requires the existence of Hall currents[86]. Applied magnetic fields might induce an azimuthal Hall current in the plasma, which in turn interacts with the radial and axial components of the applied magnetic field to produce axial ($-j_\theta B_r$) and radial ($j_\theta B_z$) body forces, which contribute to directed thrust and radial compression of the plasma. The experimental evidence for the existence of Hall currents in applied-field MPD thrusters was limited and contradictory, however, and their role in applied-field MPD thruster acceleration was uncertain[9].

Summarizing the status of MPD thruster theory in 1967, Nerheim and Kelley concluded that the level of understanding of basic MPD thruster operation was insufficient to "...allow a critical evaluation of the reported performance data, to extrapolate the performance obtained in the laboratory to that which may be expected in space, or to aid appreciably in the design of an 'optimum' engine. Thus, the full potential and the limitations of the MPD thrustor [*sic*] are not known at the present time". While the latter comment remains true, steady progress has been made in several areas of MPD thruster modeling and analysis. The status of recent MPD thruster modeling efforts, and associated issues which must be resolved, are outlined in the following sections.

Self-field MPD Thruster Models.

Several of the self-field models listed in Table 2 have been designed to investigate performance trends rather than provide specific calculations for comparison with experimental measurements. While limited in scope and detail, these models have provided necessary insight into several aspects of self-field MPD thruster operation. A few of the models have made specific predictions of such global parameters as thrust, current distribution, and voltage, which can be compared with experimental measurements. These specific comparisons and more general trends are discussed below.

Thrust.

Several recent MPD thruster models have been fairly successful in predicting self-field MPD engine thrust and thrust coefficients over a wide range of operating conditions[47,55,57,62]. Figure 9 presents measured[87] and predicted[62] thrust characteristics for the Princeton University half-scale flared anode thruster (HSFAT), plotted as a function of discharge current for various argon propellant mass flow rates. Good agreement has been obtained between the NASA LeRC single-fluid, two-dimensional model and the experimentally measured values for each of the mass flow rates and discharge currents up to $J^2/\dot{m}$ values of approximately 1.5×10^{11} A^2-s/kg, at which point the calculated thrust begins to deviate from the measured values. Thruster voltage oscillations were experimentally observed at $J^2/\dot{m}$ values around 1.8×10^{11} A^2-s/kg, and it is probable that the simple single-fluid model used in the comparison cannot accurately model the physical processes occurring in the thruster as this operational instability is approached. Good agreement between predicted and measured thrust has also been obtained by the University of Stuttgart[55] for the DT-series thrusters operated at low values of $J^2/\dot{m}$.

Figure 10 reproduces experimentally determined values of the thrust coefficient for the HSFAT as a function of $J^2/\dot{m}$ with predictions from the LeRC model overlayed on the experimental data[62]. Again, good agreement is observed between the model and the experimental measurements. Similar agreement has also been obtained using an analytic self-field model developed by Martinez-Sanchez[47]. The thrust coefficient varies from a value of approximately 7.5×10^{-7} N/A^2 at low $J^2/\dot{m}$, corresponding to a predominantly electrothermal regime of operation, to an approximately constant value of 1.1×10^{-7} N/A^2 at values of $J^2/\dot{m}$ which correspond to predominantly electromagnetic regime of thruster operation.

Current Distribution.

Predictions of steady-state anode current distributions have compared favorably with measurements performed at the University of Stuttgart using cylindrical, segmented anodes[51,55,62]. Table 3 displays the experimentally measured anode current fractions for the ZT-1 MPD thruster[88], with the current fractions predicted by the Stuttgart[51] and LeRC[62] 2-D MPD models. Good agreement is obtained between the models and the measured anode current fractions for the operating data reported (6000 amps, 6 g/s of argon). The predicted current distributions within the thruster are displayed in Fig. 11, showing similar distributions between the two models. Current distributions within the steady-state thruster could not be measured, but the agreement

with the anode current fractions lends some confidence that the predicted steady-state distributions are reasonable.

This confidence quickly erodes, however, when predicted contours are compared with actual current contours measured in quasi-steady MPD thrusters. Figure 12 displays predicted [62] and measured[87] current contours for the Princeton HSFAT, operated at 17.8 kA with an argon mass flow rate of 3 g/s. Several differences are observed between the distributions. Roughly 50% of the predicted current distribution lies within the inlet channel, compared with 30% of the actual current. The predicted current distribution is predominantly radial, while the measured current contains a significant axial component, stretching from the cathode base toward the anode tip. Similar differences occur between measured and calculated current distributions in the cylindrical Stuttgart MPD thrusters[88], and have been ascribed to variations in the cathode emission distributions between quasi-steady and steady-state operation[55,88]. Electrode processes have yet to be coupled with MPD flow models, however, and it is thus arguable whether the discrepancy between measurement and prediction lies in physical differences between quasi-steady and steady-state electrode emission processes, or in the inadequate modeling of relevant electrode phenomena. An experimental comparison of anode current distributions for a segmented anode thruster operated under quasi-steady and steady-state conditions would help to resolve this issue, and contribute to our understanding of whether quasi-steady MPD thruster data accurately reflects steady-state operating conditions.

Preliminary modeling results have been reported on the influence of the electrode geometry[43,47,52,56,95] on the self-field thruster current distribution. In general, the analyses indicate that contouring the electrode geometries may be an effective way to control the current distributions. Converging-diverging anode geometries appear to provide a more uniform current distribution along the electrodes than constant area channels, where the current tends to congregate at the inlet and exit regions of the thruster. The more uniform current attachment achieved with the converging-diverging anode geometries may help to mitigate the localized heating and associated erosion of the thruster electrodes.

Voltage.

In addition to anode current fractions, Table 3 displays the measured and predicted discharge voltages for the University of Stuttgart ZT-1 thruster. The predicted voltage drops were calculated by integrating the radial electric field from cathode to anode, excluding electrode fall voltages or sheath potentials. The Stuttgart model predicts a potential drop across the plasma of 14 volts, which is in fair agreement with the total discharge voltage of 19 volts. The LeRC model, however, predicts a potential drop of only 3.5 volts across the plasma, much lower than either the Stuttgart model prediction or the measured total voltage. The calculated plasma potential is inversely proportional to the electrical conductivity, and the discrepancy in the model predictions arises from differences in the electrical conductivities calculated in each model. The contribution of electrode fall and sheath voltages to the total discharge voltage was not measured in the steady-state device, hence it is uncertain which model more accurately reflects the actual plasma potential. Experimental measurements of anode fall voltages or plasma potentials, in conjunction with anode current distribution measurements, would allow significant refinement of current MPD thruster models and would be of tremendous aid in the development of future electrode sheath and boundary flow models.

Figure 13 displays measured total[87] and calculated plasma[62] voltage-current characteristics for the Princeton HSFAT for a variety of currents and mass flow rates. The model does not include electrode fall or sheath potentials, hence predicts a voltage substantially below the total measured discharge voltage. Nevertheless, the calculated plasma drop increases with increasing current, though at a slightly reduced rate compared with the total discharge voltage. In addition, the calculated potentials reproduce the dependence on mass flow rate observed in the total voltage measurements.

Niewood and Martinez-Sanchez[63] have recently modeled the effects of high Hall currents near constant

area MPD thruster anodes. In addition to highly skewed current contours (Fig. 8), the Hall effect leads to anode starvation and a subsequently large anode potential drop. At a discharge current of 30 kA and a mass flow rate of 4 g/s, the calculated anode fall was approximately 19 volts, out of a total calculated discharge voltage of 26 volts. Heimerdinger[52] measured a near-anode fall of 25 volts for a fully flared thruster operating under similar conditions, with a total voltage drop of approximately 40-50 volts. While the model predictions are low compared to similar experimental measurements, they indicate that at least under the reported operating conditions Hall currents may have a significant impact on the anode fall voltages. Such preliminary results should be followed up with additional experimental measurements and modeling predictions under a variety of operating conditions to establish the impact of electrode-boundary Hall terms on self-field MPD thruster performance.

Applied-field Models.

The added complexity of applied magnetic field terms in the MPD acceleration process and the abundance of self-field experimental measurements have kept the numerical modeling efforts focused primarily on self-field MPD thrusters. However, interest has been rekindled in applied-field modeling efforts by the resurgence of applied-field MPD thruster experiments.

One of the earlier treatments incorporating applied magnetic field effects with MPD thruster flow properties was published by Krulle[42], who assumed an applied-field distribution and used simplified flow equations to study electromagnetic acceleration mechanisms at low $J^2/\dot{m}$ values. It was assumed that the plasma was fully ionized, and the self-induced magnetic field was negligible in comparison with the applied magnetic field. For the operating regimes considered ($J^2/\dot{m} < 1 \times 10^{10}$ A^2 -s/kg), it was determined that a large fraction of the total thrust was due to a pressure force arising from a radially compressive $\vec{j} \times \vec{B}$ force acting on the plasma near the cathode tip. The model also showed that substantial current was carried out of the thruster and into the plume region as the applied magnetic field is increased, in qualitative agreement with experiment[89].

Fradkin[89,90] performed experimental measurements on an applied-field MPD thruster in the 10-35 kW operating range, and derived simple analytic expressions for the voltage, thrust, thrust efficiency, and thermal efficiency which were in reasonable agreement with the experimental results. Fradkin attempted to explain his measurements using the applied field torque model discussed in Nerheim and Kelly[9]. His model was incomplete, however, in that it did not include recovery of thermal energy during the expansion through the magnetic nozzle.

Tanaka and Kimura[54] analyzed applied-field acceleration mechanisms using two-dimensional electromagnetic field equations and quasi-1D fluid equations with a number of additional simplifying assumptions. They found that current distributions along the anode were strongly influenced by variations in the applied-field strengths, while current distributions along the cathode shifted from the base toward the cathode tip as the applied-field strength increased. Significant Hall currents were produced by the interactions of the discharge current with applied magnetic field. The Hall currents interacted with the applied magnetic field to produce plasma rotation, which was converted into axial momentum as the plasma expanded through the magnetic nozzle. The addition of joule heating due to the applied-field acceleration mechanism was found to be negligible for the operating regimes considered (discharge currents of 1000-2000 A, propellant mass flow of 0.1 g/s argon, axial magnetic field strengths of 0.1-0.2 T at the cathode tip).

Plasma flow through magnetic fields has long been of interest to workers in the plasma fusion energy program, whose somewhat diametric goal is to magnetically confine the plasma for as long as possible. The expertise in plasma/field interactions gained by researchers in the magnetic fusion community has recently been applied to studies of high power, high thrust, applied-field plasma thrusters for spacecraft propulsion[91]. Gerwin *et al.*[92] have modeled the flow of an ideal MHD plasma through a magnetic nozzle for a wide range of plasma densities and temperatures, and provide a detailed discussion of issues related to ideal plasma acceleration and

detachment from magnetic field lines. Detachment from magnetic field lines in the absence of meridional electric currents is analyzed by Hooper[93], who finds that separation is significantly constrained unless electric currents flow across the magnetic field.

Plasma Instability Models.

Models have been developed to investigate the causes of both macroscopic and microscopic plasma instabilities associated with MPD thruster operation. As noted in previous sections, the severe electrode erosion observed at high values of $J^2/\dot{m}$ corresponds to the onset of voltage oscillations and unsteady thruster operation. Several mechanisms have been proposed to explain the onset of these oscillations, including anode mass starvation[68], flow choking due to enhanced back-EMF[69,70], and the triggering of electrothermal and gradient-driven instabilities as the plasma approaches full ionization[13,71,72]. It appears that different operating conditions may trigger one or a combination of the proposed mechanisms, thus limiting thruster performance and lifetime.

On a less dramatic scale, plasma microinstabilities may lead to increased plasma resistivity, leading to an increase in the voltage drop and decreasing the thruster efficiency. Rempferer *et al.*[73] used a linear dispersion relation to show that electron acoustic wave instabilities are possible in MPD thrusters under normal operating conditions. Choueiri *et al.*[20,74,75] derived general nonlinear dispersion relations for current-driven plasma instabilities, and determined that lower-hybrid waves are the dominant instability for most MPD thruster operating regimes. As noted in a previous section, the existence of these waves has recently been verified in both low power and high power MPD thruster experiments[20,25].

Plasma instability models have so far been uncoupled from the plasma flow models discussed earlier. Niewoood *et al.*[94] considered the effects of microinstabilities on the thruster operating conditions using a quasi-1D fluid model[56] and a nonlinear dispersion relation for the modified two-stream instability. Plasma parameters obtained from the fluid model are used to determine whether the instability exists in a given region; if so, the anamolous collision frequency determined from the dispersion relation is used to determine new values of the ion and electron heating rates, which in turn affect the plasma flow model. The results of this iterative modeling show a slightly increased potential difference across the electrodes, with little noticeable change in the overall thruster performance. It would be of considerable interest to expand this effort by coupling other plasma microinstability models (particularly the lower hybrid instability) with a more detailed plasma flow model. This iterative approach between microinstability theory and macroscopic fluid model could provide substantial insight into the effects of plasma instabilities on MPD thruster performance.

Conclusions

Significant progress has been made in the establishment of a broad performance and lifetime database, and in the development of numerical models for MPD thrusters. Thrusters have been operated at specific impulses up to 7000 sec, at efficiencies approaching 40% and at power levels over 0.5 MW. Efforts directed at establishing empirical scaling laws for applied-field thrusters, identifying primary causes of thruster inefficiency, and establishing reasons for observed performance limitations have started to produce results which can be used to directly improve thruster performance. The observed correlations between the anode power loss, the thruster geometry, and the applied-field strength indicate that significant improvements can be obtained using appropriate anode shapes and propellant injection. The identification of the lower hybrid instability as the dominant source of plasma microtorbolence in thrusters operated over three orders-of-magnitude in power level will not only aid in the development of appropriate transport models, but also has significant implications for self-field thruster scaling.

For the first time in the last 20 years cathode erosion rates have been measured which, assuming they are constant, are low enough to achieve the required lifetimes for the missions of interest. Identification of surface temperature, propellant purity, and chamber pressure as the controlling factors for cathode erosion will

greatly aid in demonstrating long life thrusters. However, the inherent coupling between MPD thruster performance and lifetime, as exemplified by the interplay between thruster geometry, chamber pressure, and cathode material backscattering rates, has been inadequately explored.

Numerical models are approaching the degree of completeness required to obtain accurate predictions. Self-field MPD thrust values have been successfully calculated for a variety of thruster geometries over a wide range of operating conditions. Calculated anode current distributions agree well with steady-state thruster measurements, although major discrepancies are observed between calculated current profiles and measured interelectrode current distributions in quasi-steady thrusters. This disagreement between predicted and measured values may result from differences in cathode emission processes between quasi-steady and steady-state thruster operation, or may reflect the omission of relevant electrode processes (sheaths, fall potentials) in present MPD thruster models. Voltage trends are in general agreement with experimentally observed voltage-current characteristics, although again the lack of an accurate treatment of electrode fall phenomena in the fluid models precludes an exact prediction of the total discharge current. Applied-field thruster flow models are less developed than their self-field counterparts, although the effects of magnetic nozzles on flowing plasmas are under active investigation. Models have been developed to evaluate plasma microinstability effects in MPD thrusters, and to predict conditions leading to the onset of thruster voltage oscillations and subsequent electrode erosion. While significant work remains to be done, a basic understanding of the "full potential and limitation" of the MPD thruster is progressing via the combined development of experimental and numerical techniques.

Acknowledgements

The authors would like to thank Scharlene Schmidt for her patient assistance in preparing the manuscript.

References

1. Hack, K. J., George, J. A., and Dudzinski, L. A., "Nuclear Electric Propulsion Mission Performance for NASA Missions," AIAA 91-3488, Sept. 1991.

2. Gilland, J.H., Myers, R.M., and Patterson, M.J., "Multimegawatt Electric Propulsion System Design Considerations," AIAA 90-2552, July 1990.

3. Hack, K. J., George, J. A., Riehl, J. P., and Gilland, J. H., "Evolutionary Use of Nuclear Electric Propulsion," AIAA 90-3821, Sept. 1990.

4. Uematsu, K., Mori, K., Kuninaka, H., and Kuriki, K., "Effects of Electrode Configuration on MPD Arcjet Performance," 17th International Electric Propulsion Conference, Japan Society for Aeronautical and Space Sciences, Tokyo, 1984, pp.79-86.

5. Connolly, D.J., Sovie, R.J., Michels, C.J., and Burkhart, J. A., "Low Environmental Pressure MPD Arc Tests," AIAA Journal, vol. 6, No. 7, July 1968, pp.1271-1276.

6. Esker, D.W., Checkley, R.J., and Kroutil, J.C., "Radiation Cooled MPD Arc Thruster," McDonnel-Douglas Corp., St. Louis, MO, MDC-H296, July 1969; see also NASA CR-72557, July 1969.

7. Sovey, J. S. Vetrone, R. H., Grisnik, S., Myers, R. M., and Parkes, J. E., "Test Facility Requirements for High Power Electric Propulsion," AIAA 91-3499, Oct. 1991.

8. Myers, R.M., "Applied-Field MPD Thruster Geometry Effects," AIAA 91-2342, June 1991.

9. Nerheim, N.M., and Kelly, A.J., "A Critical Review of the Magnetoplasmadynamic (MPD) Thruster for Space Applications," Jet Propulsion Lab., California Institute of Technology, Pasadena, CA, JPL-TR-32-1196, Feb. 1968; see also NASA CR-93139, Feb. 1968.

10. Sovey, J. S. and Mantenieks, M.A., "Performance and Lifetime Assessment of Magnetoplasmadynamic Arc Thruster Technology," Journal of Propulsion and Power, Vol. 7, No. 1, Jan.-Feb. 1991, pp.71-83.

11. Haag, T. W., "Thrust Stand for High-Power Electric Propulsion Devices," Rev. Sci. Instrum. 62 (5), May, 1991; see also NASA TM 102372, July 1989.

12. Barnett J. W., "Operation of the MPD Thruster with Stepped Current Input," Ph.D. Thesis, Dept. of Mech. and Aero. Engineering, Princeton University, April 1985.

13. Preble, J.C., "Onset in Magnetoplasmadynamic Thrusters: A Model of an Electrothermal Instability," M.S. Thesis, Dept. of Aero. and Astro., Massachussets Inst. of Technology, May, 1990.

14. Gallimore, A. D., Kelly, A. J., and Jahn, R. G., "Anode Power Deposition in Quasi-Steady MPD Thrusters, "AIAA 90-2668, July 1990.

15. Gallimore, A. D., Myers, R. M., Kelly, A. J., and Jahn R. G., "Anode Power Deposition in an Applied-field Segmented Anode MPD Thrusters," AIAA 91-2343, June, 1991.

16. Myers, R. M., Kelly, A. J., and Jahn, R. G., "Energy Deposition in Low Power Coaxial Plasma Thrusters," IEPC 88-024, presented at 20th International Electric Propulsion Conference, W. Germany, Oct. 1998.

17. Myers R. M., Suzuki N., Kelly A. J., and Jahn R. G., "Cathode Phenomena in a Low Power, Steady State MPD Thruster," AIAA - 88-3206, July 1988.

18. Auweter-Kurtz, M., and Messerschmid, E., "Plasma Accelerator Activities at the IRS," AIAA 90-2659, 21st Intern. Electric Propulsion Conference, July 1990.

19. Turchi, P., "The Cathode Region of a Quasi-Steady Magnetoplasmadynamic Arcjet," PhD. Thesis, Dept. of Mech. and Aero. Engineering, Princeton University, Princeton, N.J., Oct 1970.

20. Choueiri, E. Y., "Electron-Ion Streaming Instabilities of an Electromagnetically Accelerated Plasma", Ph.D. dissertation, Mechanical and Aerospace Engineering Department, Princeton University, Princeton, NJ, Sept. 1991.

21. Sasoh, A., Solem, A. T., and Arakawa, Y., "Optimization of Current Distribution in an Applied Field MPD Thruster," IEPC 88-057, 20th Intern. Electric Propulsion Conference, Garmisch - Partenkirchen, Oct. 1988.

22. Merke, W. D., Auweter-Kurtz, M., Habiger, H., Kurtz, H., and Schrade, H. O.,"Nozzle Type MPD Thruster Experimental Investigations," IEPC 88-028, 20th Intern. Electric Propulsion Conference, Garmisch-Partenkirchen, W. Germany Oct. 1988.

23. Tahara H., Sasaki M., Kagaya Y. and Yoshikawa T.,"Thruster Performance and Acceleration Mechanisms of a Quasi-Steady Applied-field MPD Arcjet," AIAA 90-2554, July 1990.

24. Mantenieks, M. A., Sovey, J. S., Myers R. M., Haag, T. W., Raitano, P., and Parkes, J. E., "Performance of a 100 kW Class Applied Field MPD Thrusters," AIAA 89-2710 July 1989, see also NASA TM 102312.

25. Tilley, D. L., "An Investigation of Microinstabilities in a kW Level Self-Field MPD Thruster," M. S. Thesis No. 1917-T, Department of Mechanical and Aerospace Engineering, Princeton University, Princeton,NJ, October 1991.

26. Wegmann, T., Auweter-Kurtz, M., Kurtz, H., Merke, W., Loesmer, O., and Schrade, H.O.,"Steady-State High Pow MPD Thrusters," AIAA 90-2555, July 1990.

27. Ohtsuka T. Vematsu, K., and Kuriki, K., " Investigations on MPD Arcjet with Projected Anodes," IEPC 88-110, 20th Intern. Electric Propulsion Conference, Grarmisch-Partenkirchen, W. Germany, Oct. 1988.

28. Tahara, H., Kagaya, Y., and Yoshikawa, T., "Hybrid MPD Thruster with Axial and Cusp Magnetic Fields," IEPC 88-058, 20th Intern. Electric Propuslion Conference, Garmish-Partenkirchen, W. Germany, Oct. 1988.

29. Yoshikawa T. Kagaya, Y, Tahara, H., and Wasa, T., "Continuous Operation of a Quasi-Steady MPD Thruster Propulsion System with an External Magnetic Field," IEPC 88-056, 20th Intern. Electric Propulsion Conference, Garnish-Partenkirchen, W. Germany, Oct. 1988.

30. Nishida, E., Shimizu, Y., and Kuriki, K., "Improved Thrust Generation Mechanism for Electrothermal/Electromagnetic Arcjet," IEPL 88-026, 20th Intern. Electric Propulsion Conference, Garmish-Partenkirchen, W. Germany, Oct. 1988.

31. Schrade, H. O., Auweter-Kurtz, M., and Kurtz, H. L.,"Cathode Phenomena in Plasma Thrusters," AIAA 87-1096, May 1987.

32. Chamberlain, F. R., "Electropositive Surface Layer MPD Thruster Cathodes, M.S. Thesis. No. 1860-T, Dept. of Mechanical and Aerospace Engineering, Princeton University, May 1989.

33. Auweter-Kurtz M., Glocker B., Kurtz H. L., Loesener O., Schrade H. O., Tubanos N., Wegmann T., "Cathode Phenomena in Plasma Thrusters" AIAA 90-2662, July 1990.

34. Schrade H. O., Auweter-Kurtz M., and Kurtz H. L., "Cathode Erosion Studies on MPD Thrusters," AIAA - 90-2659, July 1990.

35. Polk J. E., Kelly A. J., and Jahn R. G., "Mechanisms of Hot Cathode Erosion in Plasma Thrusters," AIAA - 90-2673, July 1990.

36. Polk J. E.,Kelly A. J., and Jahn R. G.,"Erosion Processes," IEPC - 88-075, presented at 20th Intern. Electric Propulsion Conference,Garmish-Pertenkirchen, W. Germany, Oct. 1988.

37. Kristiansen, M., and Hatfield, L., Workshop Co-Chairmen "Electrode Erosion in Electric Space Propulsion Engines,"Texas Tech Univ., Lubbock, Texas, May 1989. p. 162.

38. Schrade, H. O., Auweter-Kurtz, M., and Kurtz, H. L., "Cathode Erosion Studies on MPD Thrusters," AIAA 85-2019, Sept. 1985.

39. Shimizu Y., Toki K., and Kuriki K., "Development of an MPD Propulsion System," AIAA - 88-015, 20th Intern. Electric Propulsion Conference, Garmisch-Partenkirchen, W. Germany, Oct. 1988.

40. Hughes, W. F. and Young, F. J., The Electrodynamics of Fluids, J. Wiley and Sons, Inc., New York, York, 1966.

41. Sutton, G. W., and Sherman, A., Engineering Magnetohydrodynamics, J, McGraw-Hill Book Co., New York, 1965.

42. Krulle, G., "Theoretical Treatment of Current, Mass Flow, and Related Distributions in MPD Plumes," AIAA Paper No. 72-501.

43. Kuriki, K., Kunii, Y., and Shimizu, Y., "Idealized Model for Plasma Acceleration in an MHD Channel," AIAA Journal, Vol. 21, No. 3, March 1983, pp. 322-326.

44. Minakuchi, H. and Kuriki, K., "Magnetoplasmadynamic Analysis of Plasma Acceleration," IEPC Paper No. 84-06, 17th International Electric Propulsion Conference, Tokyo, Japan, May 28-31, 1984.

45. Kurtz, H. L., Auweter-Kurtz, M., and Schrade, H. O., "Self-field MPD Thruster Design - Experimental and Theoretical Investigations," AIAA 85-2002, Oct. 1985.

46. Yamada, H. and Fujiwara, T., "Computational Fluid Dynamics Study of an MPD Thruster," Memoirs of the Faculty of Engineering, Nagoya University, Japan, Vo. 38 No. 2, 1986, pp. 261-278.

47. Martinez-Sanchez, M., "Structure of Self-Field Accelerated Plasma Flows," J. Propulsion and Power, 7(1), Jan.-Feb. 1991, pp. 56-64; also published as AIAA 87-1065, May 1987 .

48. Chanty, J. M. G. and Martinez-Sanchez, M., "Two Dimensional Numerical Simulation of MPD Flows," AIAA 87-1090, May 1987.

49. Tahara, H., Yasui, H., Kagaya, Y., and Yoshikawa, T., "Experimental and Theoretical Researches on Arc Structure in a Self-Field Thruster," AIAA 87-1093, May 1987.

50. Park, W. and Choi, D.,"Numerical Analysis of MPD Arcs for Plasma Acceleration," IEEE Tansactions on Plasma Science, PS- 15 (5), October 1987, pp. 618-624.

51. Sleziona, P. C., Auweter-Kurtz, M., and Schrade, H. O., "Numerical Codes for Cylindrical MPD Thrusters," IEPC 88-038, presented at the 20th International Electric Propulsion Conference, Garmisch-Partenkirchen, West Germany, October 3-6, 1988.

52. Heimerdinger, D. J. and Martinez-Sanchez, M., "Fluid Dynamics in a Magnetoplasmadynamic Thruster," IEPC 88-039, presented at the 20th International Electric Propulsion Conference, Garmisch-Partenkirchen, West Germany, October 3-6, 1988.

53. Auweter-Kurtz, M., Glaser, S. F., Kurtz, H. L., Schrade, H. O., and Sleziona, P. C., "An Improved Code for Nozzle Type Steady State MPD Thrusters," 88-040, presented at the 20th International Electric Propulsion Conference, Garmisch-Partenkirchen, West Germany, October 3-6, 1988.

54. Tanaka, M. and Kimura, I., "Current Distribution and Plasma Acceleration in MPD Arcjets with Applied Magnetic Fields," J. Propulsion and Power, 4(5), Sept.-Oct. 1988, pp. 428-436.

55. Sleziona, P. C., Auweter-Kurtz, M., and Schrade, H. O., "Numerical Evaluation of MPD Thrusters,"

AIAA-90-2602, July 1990.

56. Niewood, E. H. and Martinez-Sanchez, M., "Quasi One-Dimensional Numerical Simulation of Magnetoplasmadynamic Thrusters," AIAA 90-2604, July 1990.

57. Sleziona, P. C., Auweter-Kurtz, M., Schrade, H. O., and Wegmann, T., "Comparison of Numerical and Experimental Investigations of Nozzle Type MPD Accelerators," AIAA 90-2663, July 1990.

58. Turchi, P. J., Davis, J. F., and Roderick, N. F., "MPD Thrust Chamber Flow Dynamics," AIAA 90-2664, July 1990.

59. Morozov, A. I., "Principles of Coaxial (Quasi-)Steady-State Plasma Accelerators," Sov. J. Plasma Phys., Vol. 16 No.2, Feb. 1990, pp.69-78.

60. Brushlinskii, K. V., Zaborov, A. M., Kozlov, A. N., Morozov, A. I., and Savel'ev, V. V., "Numerical Modeling of Plasma Flow in High-Current Quasistationary Plasma Accelerators," Sov. J. Plasma Phys., Vol.16 No. 2, Feb. 1990, pp. 79-85.

61. Caldo, G., "An Improved Numerical Study of MPD Thruster Physics," Princeton University Physics Department Undergraduate Thesis, April 1991.

62. LaPointe, M. R., "Numerical Simulation of Self-Field MPD Thrusters," July 1991; AIAA Paper No. 91-2341, also see NASA CR 187168, August 1991.

63. Niewood, E. H. and Martinez-Sanchez, M., "A Two Dimensional Model of an MPD Thruster," AIAA 91-2344, July 1991.

64. Myers, R. M., "Energy Deposition in Low Power Coaxial PlasmaThrusters," Ph. D. Thesis No. 1859-T, Department of Mechanical and Aerospace Engineering, Princeton University, Princeton, NJ, June 1989.

65. Goodfellow, K. D. and Murthy, S. N. B., "Cathode Processes in a MPD Arcjet," IEPC 88-072, presented at the 20th International Electric Propulsion Conference, Garmisch-Partenkirchen, West Germany, October 3-6, 1988.

66. Godyak, V. A. and Sternberg, N., "Smooth Plasma-Sheath Transition in a Hydrodynamic Model," IEEE Transactions on Plasma Science, Vol. 18 No. 1, Feb. 1990, pp. 159-168.

67. Subramaniam, V. V. and Lawless, J. L., "Electrode-Adjacent Boundary Layer Flow in Magnetoplasmadynamic Thrusters," Phys. Fluids, Vo.31 No.1, Jan. 1988, pp. 201-209.

68. Hugel, H., "Effect of Self-Magnetic Forces on the Anode Mechanism of a High Current Discharge," IEEE Transactions on Plasma Science, PS-4(4), December 1980, pp. 437-442.

69. Lawless, J. L., and Subramaniam, V. V., "Theory of Onset in Magnetoplasmadynamic Thrusters," J. Propulsion and Power, Vol. 3 No. 2, March-April 1987, pp. 121-127.

70. Subramaniam, V. V. and Lawless, J. L., "Onset in Magnetoplasmadynamic Thrusters with Finite-Rate

Ionization," J. Propulsion and Power, 4(6), Nov.-Dec. 1988, pp. 526-532.

71. Wagner, H. P., Auweter-Kurtz, M., Roesgen, T., Messerschmid, E. W., and Kaeppeler, H. J., "Gradient Driven Instabilties in Stationary MPD Thruster Flows," AIAA 90-2603, July 1990.

72. Smith, J. M., "Electrothermal Instability - An Explanation of the MPD Thruster Rotating Spoke Phenomenon," AIAA 69-231, May 1969.

73. Rempfer, D., Auweter-Kurtz, M., Kaeppeler, H. J., and Maurer, M., "Investigation of Instabilities in MPD Thruster Flows Using a Linear Dispersion Relation," IEPC 88-071, presented at the 20th International Electric Propulsion Conference, Garmisch-Partenkirchen, West Germany, October 3-6, 1988.

74. Choueiri, E. Y., Kelley, A. J., and Jahn. R. G., "MPD Thruster Plasma Instability Studies," AIAA 87-1067, May 1987.

75. Choueiri, E. Y., Kelley, A. J., and Jahn, R. G., "Current Driven Instabilities of an Electromagnetically Accelerated Plasma," IEPC Paper No. 88-042, presented at the 20th International Electric Propulsion Conference, Garmisch-Partenkirchen, West Germany, October 3-6, 1988.

76. Seals, R. K. and Hassan, H. A., "Analysis of MPD Arcs with Nonequilibrium Ionization," AIAA Journal, Vol. 8 No. 12, December 1968, pp. 2273-2278.

77. Shoji, T. and Kimura, I., "Analytical Study on the Influence of Nonequilibrium Ionization for Current Flow Pattern and Flow Field of MPD Arcjet," AIAA 90-2609, July 1990.

78. Sheppard, E. J. and Martinez-Sanchez, M., "Nonequilibrium Ionization in Plasma Accelerators," AIAA 90-2608, July 1990.

79. Sheppard, E. J., Chanty, J. M. G., and Martinez-Sanchez, M., "Local Analysis in MPD Thrusters: Diffusion-Reaction and Magnetodynamic Regimes," AIAA 91-2589, July 1990.

80. Kilfoyle, D. B., Martinez-Sanchez, M., Heimerdinger, D. J., Sheppard, E. J., "Spectroscopic Investigation of the Exit Plane of an MPD Thruster," IEPC 88-027, presented at the 20th International Electric Propulsion Conference, Garmisch-Partenkirchen, West Germany, October 3-6, 1988.

81. Miller, S. and Martinez-Sanchez, M., "Viscous and Diffusive Effects in MPD Flows," AIAA 90-2606, July 1990.

82. Maecker, H., "Plasmastronmugen in Lichtobogen infloge eigen Magnetioischer Kompression," Z. Phys., 141, 1955, pp. 198.

83. Jahn, R. G., Physics of Electric Propulsion, McGraw-Hill Book Co., New York, 1968, pp. 240-246.

84. Ducati, A. C., Jahn, R. G., Muehlberger, E., and Treat, R. P., "Design and Development of a Thermolonic Electric Thrustor," NASA CR-54703, May 1966.

85. Rosciszewski, J., "Acceleration Process in the Hall Current Device," Phys. Fluids, Vol. 10 No. 5, May 1967, pp. 1095-1099.

86. Cann, G. L., Harder, R. L., Moore, R. A., and Lenn, P. D., "Hall Current Accelerator," NASA CR-

54705, February 1966.

87. Gilland, J. H., "The Effect of Geometrical Scale Upon MPD Thruster Behavior," M. S. Thesis No. 181 1-T, Department of Mechanical and Aerospace Engineering, Princeton University, Princeton, NJ, March 1988.

88. Kurtz, H. L., Auweter-Kurtz, M., Glocker, B., Habiger, H., Merke, W., and Schrade, H. 0., "Cylindrical Steady-State MPD Thruster," IEPC 88-025, presented at the 20th International Electric Propulsion Conference, Garmisch-Partenkirchen, West Germany, October 3-6, 1988.

89. Fradkin, D. B., Blackstock, A. W., Roehling, D. J., Stratton, T. F., Williams, M., and Liewer, K. W., "Experiments Using a 25-kW hollow Cathode Lithium Vapor MPD Arcjet," AIAA Journal Vol. 8 No. 5, May 1970, pp. 886-894.

90. Fradkin, D. B., "Analysis of Acceleration Mechanisms and Performance of an Applied Field MPD Arcjet," Ph.D. Dissertation No. 1088-T, Department of Mechanical and Aerospace Engineering, Princeton University, Princeton, NJ, March 1973.

91. Gerwin, R. A., Schoenberg, K. F., and Rej, D. J., "Preliminary Scoping Studies for Nozzle-Based Coaxial Plasma Thrusters," Proceedings of the Eighth Symposia on Space Nuclear Power Systems, January 6-10, 1991, Albuquerque, NM, pp.493-500.

92. Gerwin, R. A., Marklin, G. J., Sgro, A. G., and Glasser, A. H., "Characterization of Plasma Flow Through Magnetic Nozzles," AL-TR-89-092, Astronautics Laboratory (AFSC), Edwards Air Force Base, CA 93523-5000, February 1990.

93. Hooper, E. B., "Plasma Detachment from a Magnetic Nozzle," AIAA 91-2590, July 1990.

94. Niewood, E. H., Preble, J., Hastings, D. E., and Martinez-Sanchez, M., "Electrothermal and Modified Two Stream Instabilities in MPD Thrusters," AIAA 90-2607, July 1990.

95. King, D. Q., "Magnetoplasmadynamic Channel Flow for Design of Coaxial MPD Thrusters," Ph.D. Dissertation No. 1544-T, Department of Mechanical and Aerospace Engineering, Princeton University, Princeton, NJ, December 1981.

Table 1: Recent Measurement of MPD Cathode Erosion Rates

Cathode Impregnant*	Propellant	Mode of Operation**	Erosion Rate (μg/C)	Comments	Ref.
2% ThO_2	Ar	S.S.	$(1.5\text{-}5.4)\times10^{-3}$	U. C. P.	18,33
		S.S.	1.8×10^{-1}	Low power (< 30kW)	17
		S.S.	3.0×10^{-2}		31
1% ThO2		S.S.	$(1.6 - 4.9)\times10^{-3}$	U. C. P.	35
2% ThO_2		S.S.	1.9×10^{-3}	U. C. P.	33
	N_2	S.S.	$(5.0\text{-}6.0)\times10^{-4}$	U. C. P.	18
	H_2	S.S.	$(6\text{-}20)\times10^{-4}$	U. C. P.	18
	N_2+2H_2	S.S.	1.3×10^{-3}	U. C. P.	18
?		Q.S.S.	6.0×10^{-1}	25 days accumulated life	39
		Q.S.S.	8.0 - 13.0	Applied B Field	23
BaO	N_2+2H_2	Q.S.S.	$(2\text{-}4)\times10^{-1}$	Self and Applied B Field	29
2%ThO_2	Ar	Q.S.S.	1-60		36

* Base material is tungsten

**S.S. = steady state

Q.S.S. = quasi-steady state

U.C.P. = ultra clean propellant

MPD THRUSTER MODEL APPROXIMATIONS		REFERENCE #																				
		42	43	44	45	46	47	48	49	50	51	52	53	54	55	56	57	58	59	60	61	62	63
PLASMA SPECIES	SINGLE FLUID	•	•	•	•	•	•	•	•	•	•	•	•	•	•		•	•			•	•	
	MULTI - SPECIES															•			•	•			•
PLASMA TEMPERATURE	SINGLE-TEMP.	•	•	•	•	•	•	•	•	•	•	•		•				•				•	
	MULTI-TEMP				•								•		•	•	•		•	•	•		•
IONIZATION PROCESSES	FULLY IONIZED	•	•	•	•	•	•	•	•	•	•	•	•	•	•		•	•	•		•	•	
	RATE EQUATIONS															•				•			•
MISCELLANEOUS PLASMA PROPERTIES	HALL EFFECT	•		•	•	•		•		•	•	•	•	•	•		•	•		•	•	•	•
	VISCOSITY									•					•	•						•	
	THERMAL COND			•						•			•		•	•	•	•			•	•	
	ION SLIP									•						•							
MAGNETIC FIELD INTERACTIONS	SELF-FIELD		•	•	•	•	•	•	•	•	•	•	•		•	•	•	•	•		•	•	•
	APPLIED-FIELD	•												•						•			
FLOW MODEL	ID				•				•				•										
	QUASI-ID		•	•			•							•		•	•						
	2D-PLANAR									•		•											•
	2D-CYLINDRICAL					•		•			•				•			•	•	•	•	•	
MPDT OPERATING REGIME MODELED	ELECTROTHERMAL	•			•		•	•		•	•		•		•		•				•	•	
	ELECTROMAGNETIC		•	•		•	•		•	•		•		•		•		•	•	•		•	•

Table 2. Recent MPD thruster models.

ZT-1 THRUSTER ANODE SEGMENT #	U. STUTTGART EXPERIMENT	U. STUTTGART MODEL	NASA LERC MODEL
	ANODE CURRENT FRACTION		
1	0.46	0.44	0.47
2	0.27	0.27	0.23
3	0.27	0.29	0.30
	DISCHARGE VOLTAGE (V)		
VOLTAGE (V)	19 V	14 V	3.7 V

Table 3. Current distribution and discharge voltage comparisons for the ZT-1 MPD thruster operating at 6000 A, 6 g/s. Calculated voltages do not include electrode fall potentials.

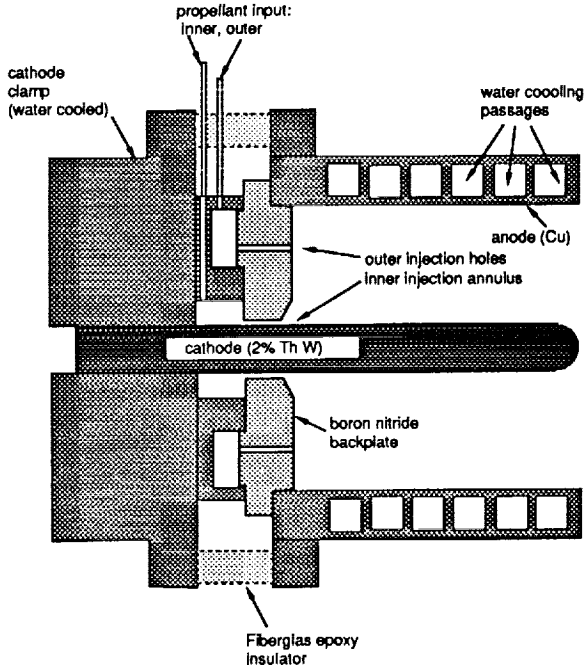

a. Steady-state applied-field thruster. Magnet (not shown) goes around outside of anode (Ref. 8).

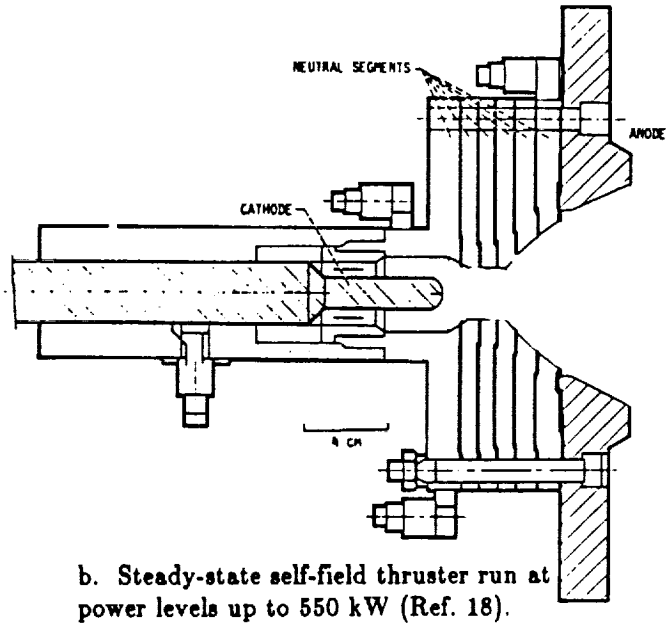

b. Steady-state self-field thruster run at power levels up to 550 kW (Ref. 18).

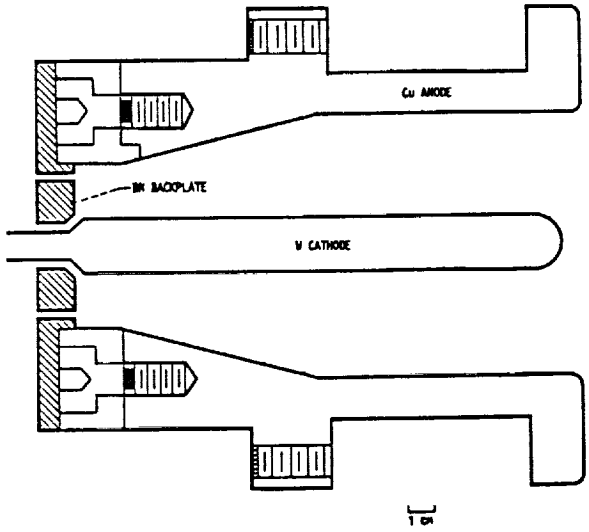

c. Half-scale flared anode (HSFAT) quasi-steady thruster run at power levels up to 5 MW (Ref. 87).

Figure 1. Schematics of typical MPD thrusters tested since 1987.

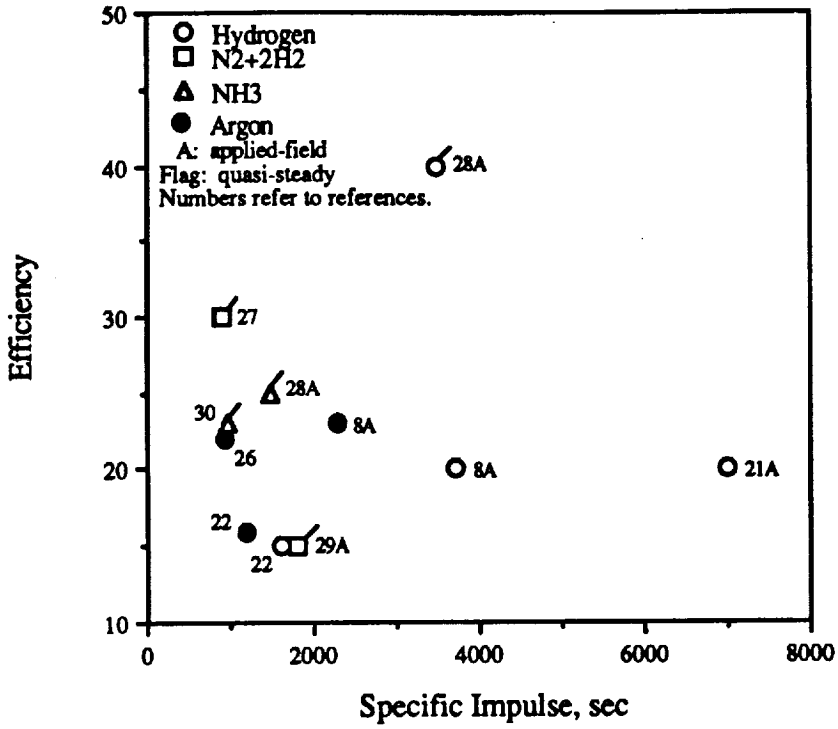

Figure 2. Peak efficiency - specific impulse values reported since 1987.

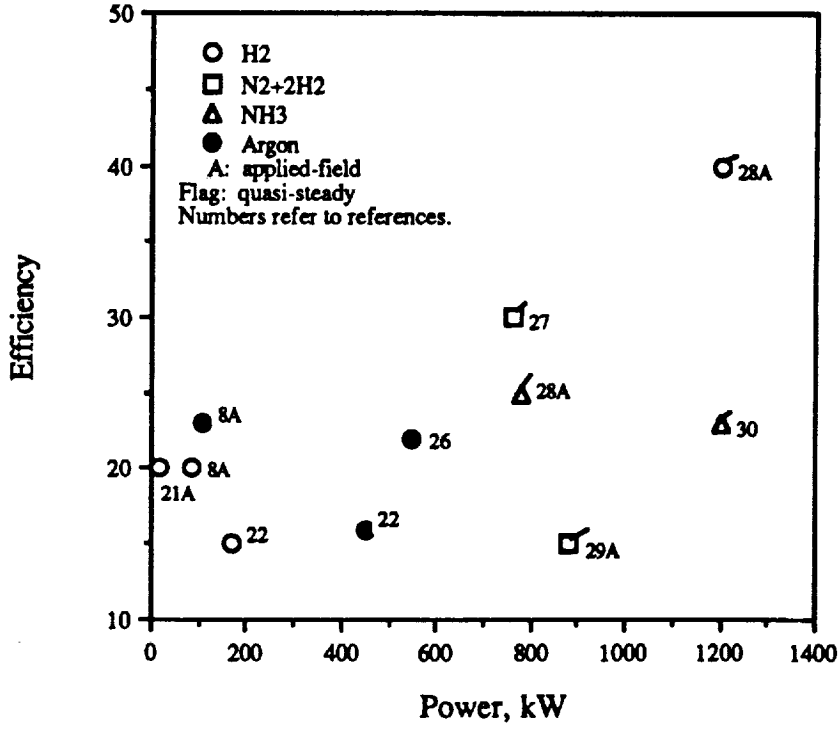

Figure 3. Peak efficiencies vs. thruster power level for data reported since 1987.

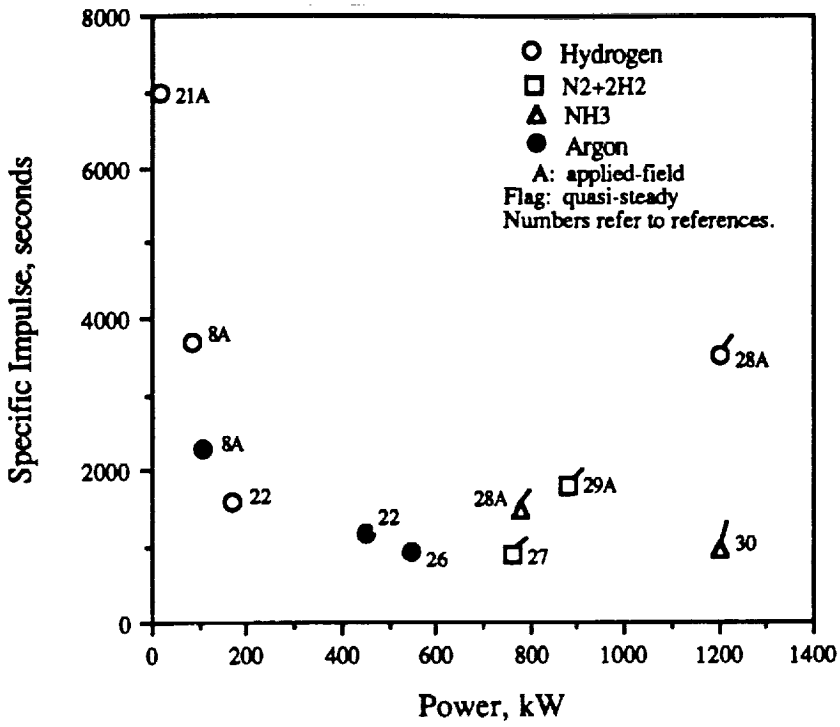

Figure 4. Peak specific impulse vs. thruster power level for measurements reported since 1987.

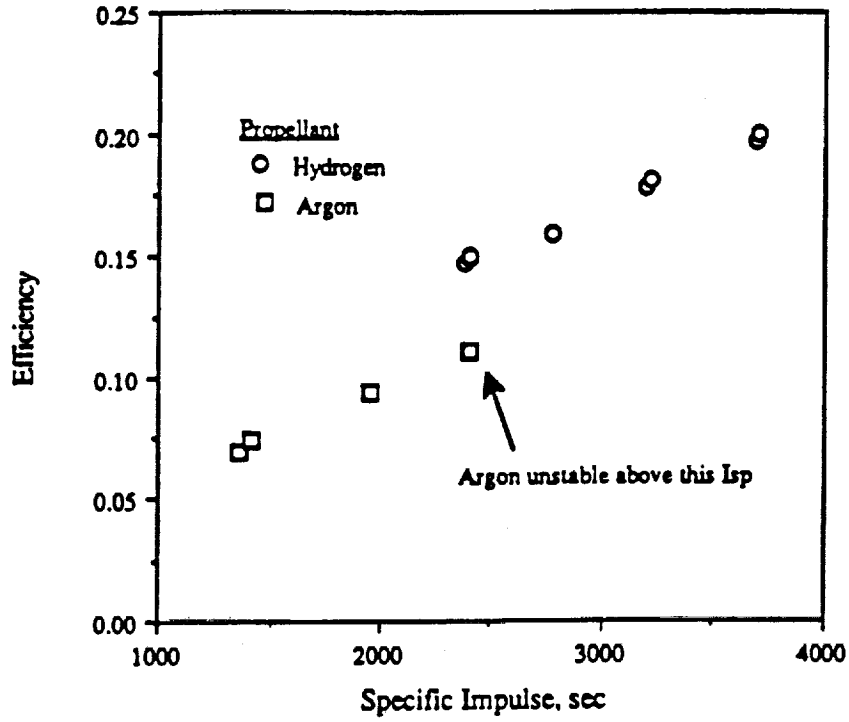

Figure 5. Comparison of performance levels obtained using hydrogen and argon propellants. Thruster geometry shown in Fig. 1a, propellant flow rate of 25 mg/s, discharge current of 750A.

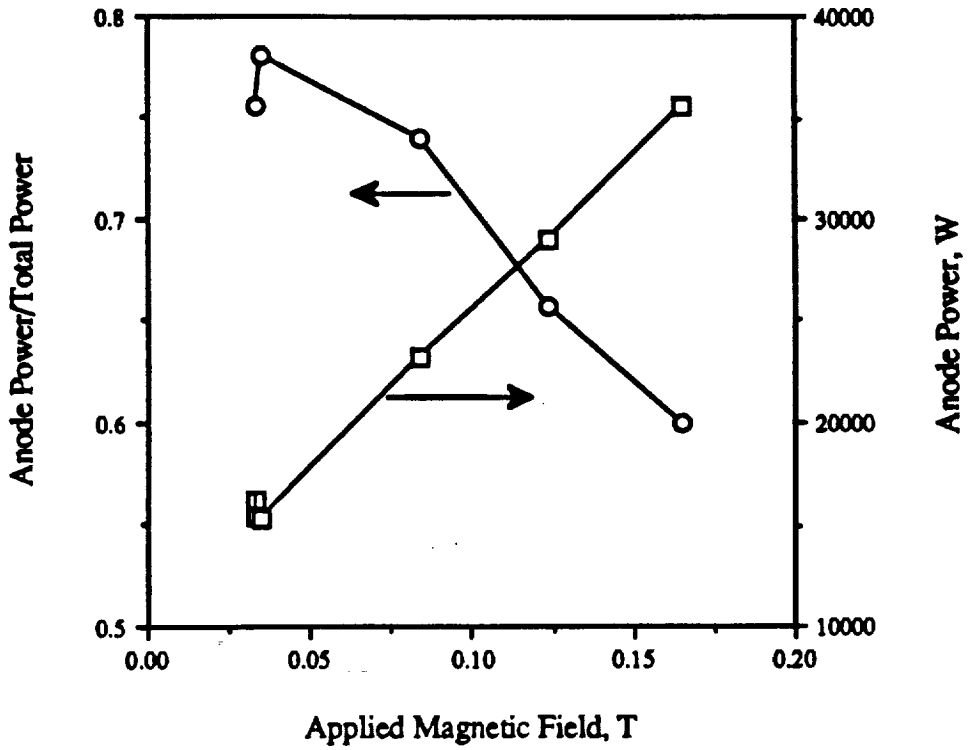

Figure 6. Anode power fraction and total anode power vs. applied magnetic field strength. Thruster geometry shown in Fig. 1a, 0.1 g/s argon propellant, discharge current of 1000A.

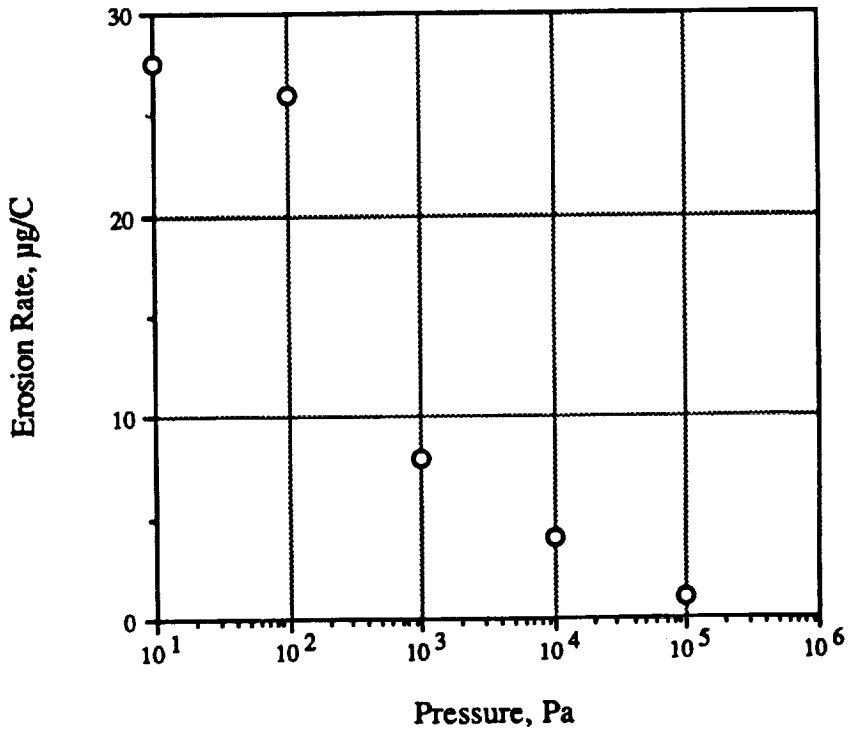

Figure 7. Erosion rate as a function of the ambient pressure of a 2% thoriated tungsten cathode in a nitrogen atmosphere (Ref 33).

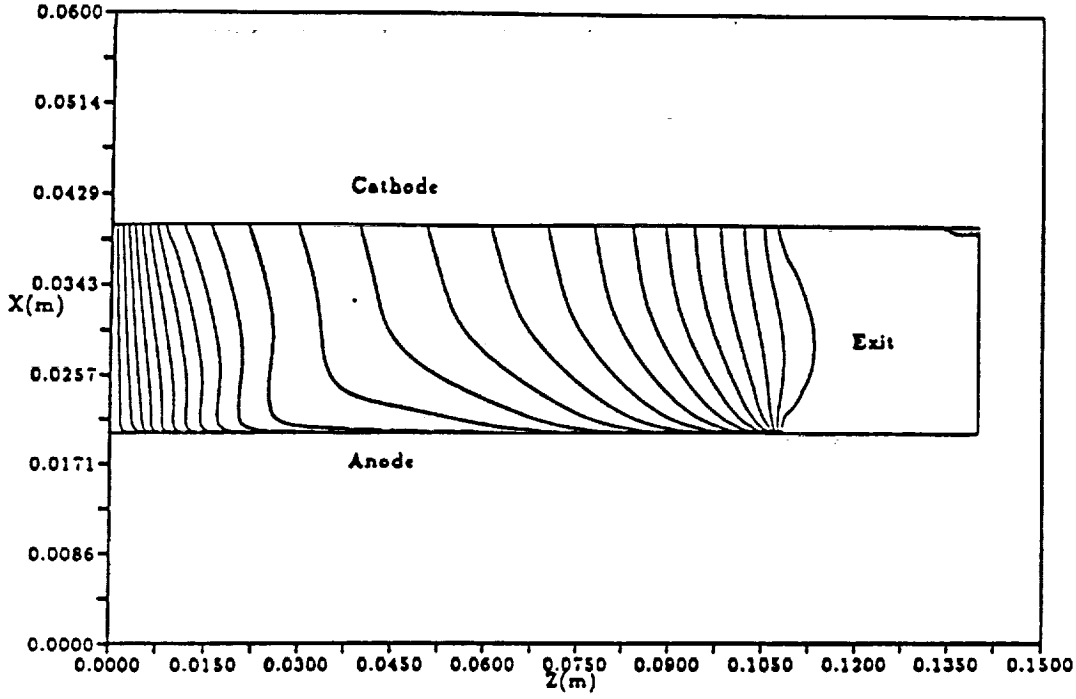

Figure 8. Theoretical current contour lines showing strong Hall effect near electrodes. Planar geometry thruster, 31 kA, 4 g/s argon propellant. Adapted from Ref. 63.

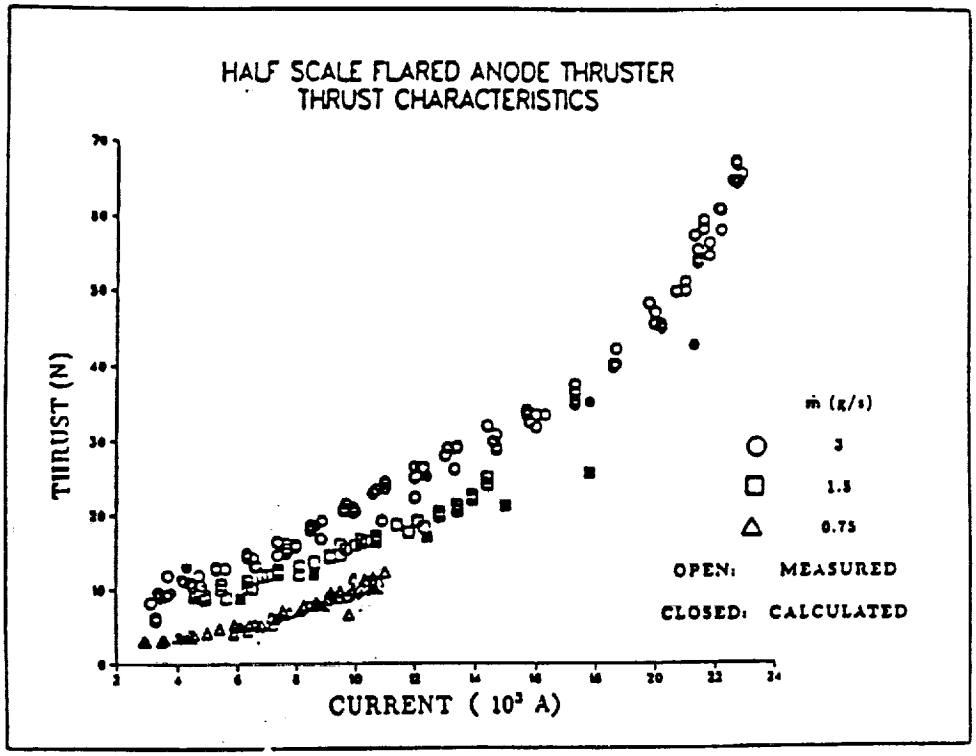

Figure 9. HSFAT thrust characteristics, argon propellant (Ref. 62).

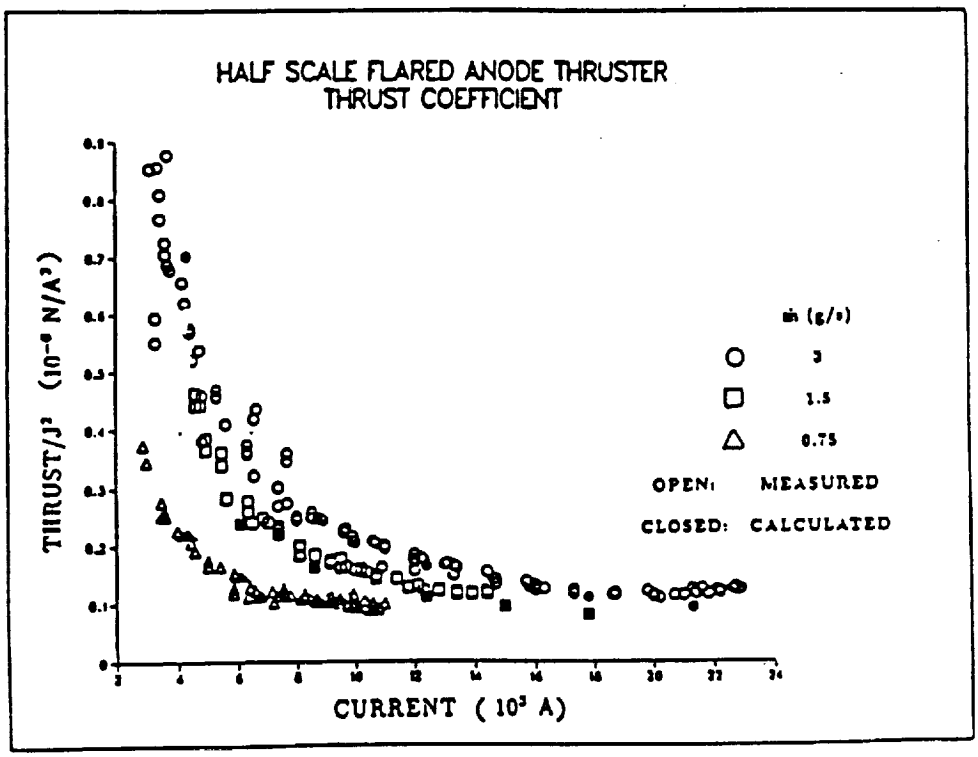

Figure 10. HSFAT thrust coefficients, argon propellant (Ref. 62).

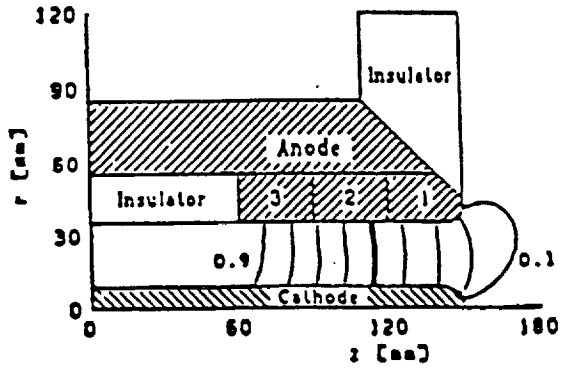

a. Enclosed current predictions from Ref. 88.

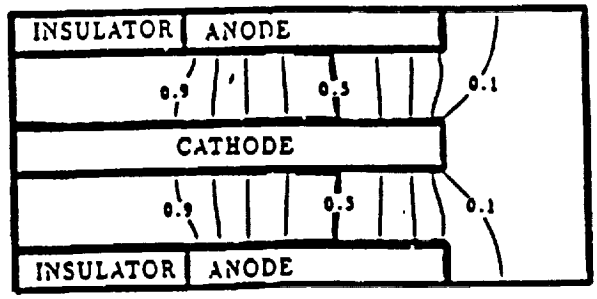

b. Enclosed current predicitions from Ref. 62.

Figure 11. Predicted enclosed current contour comparisons for the ZT-1 thruster operating at 6000 A, 6 g/s, argon propellant. Contour levels every 10%.

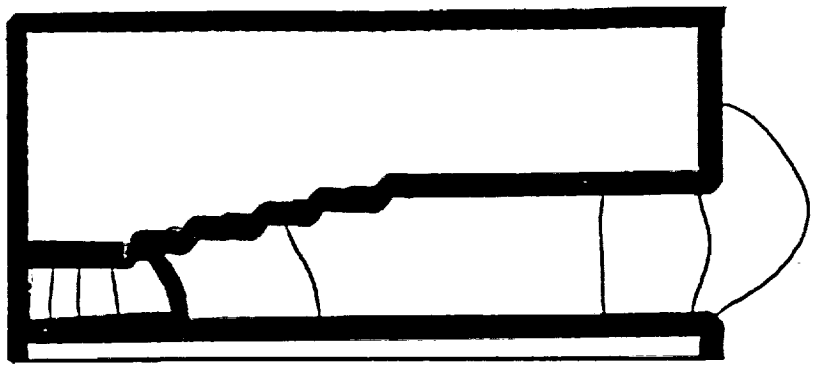

a. Predictions from Ref. 62.

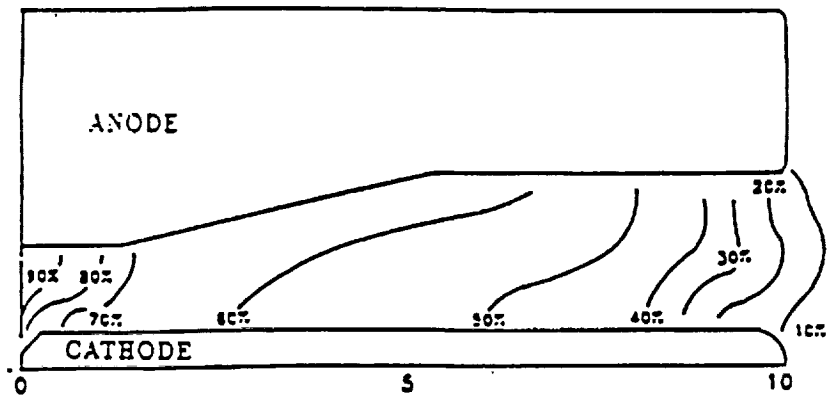

b. Measurements from Ref. 87.

Figure 12. Comparison of predicted steady-stated and measured quasi-steady current distributions. HSFAT thruster, 3 g/s argon, 17.8 kA discharge current.

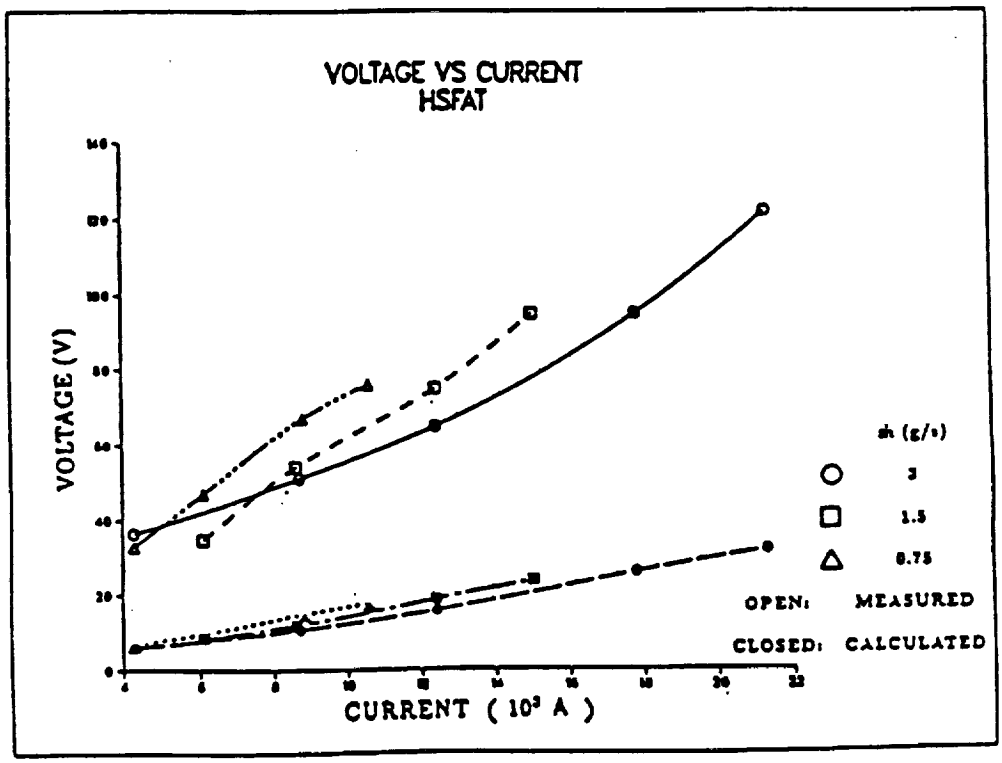

Figure 13. Measured total voltage and predicted plasma voltage vs. current for the HSFAT thruster. Argon propellant.

REPORT DOCUMENTATION PAGE

Form Approved
OMB No. 0704-0188

1. AGENCY USE ONLY (*Leave blank*)	2. REPORT DATE	3. REPORT TYPE AND DATES COVERED
	September 1991	Technical Memorandum

4. TITLE AND SUBTITLE
MPD Thruster Technology

5. FUNDING NUMBERS
WU - 506 - 42 - 31

6. AUTHOR(S)
Roger M. Myers, Maris A. Mantenieks, and Michael R. LaPointe

7. PERFORMING ORGANIZATION NAME(S) AND ADDRESS(ES)
National Aeronautics and Space Administration
Lewis Research Center
Cleveland, Ohio 44135 - 3191

8. PERFORMING ORGANIZATION REPORT NUMBER
E - 6569

9. SPONSORING/MONITORING AGENCY NAMES(S) AND ADDRESS(ES)
National Aeronautics and Space Administration
Washington, D.C. 20546 - 0001

10. SPONSORING/MONITORING AGENCY REPORT NUMBER
NASA TM - 105242
AIAA - 91 - 3568

11. SUPPLEMENTARY NOTES
Prepared for the Conference on Advanced Space Exploration Initiative Technologies cosponsored by AIAA, NASA, and OAI, Cleveland, Ohio, September 4 - 6, 1991. Roger M. Myers and Michael R. LaPointe, Sverdrup Technology, Inc., NASA Lewis Research Center Group, 2001 Aerospace Parkway, Brook Park, Ohio 44142 (work funded under NASA Contract NAS3 - 25266). Maris A. Mantenieks, NASA Lewis Research Center. Responsible person, Roger M. Myers, (216) 433 - 8548.

12a. DISTRIBUTION/AVAILABILITY STATEMENT
Unclassified - Unlimited
Subject Category 20

12b. DISTRIBUTION CODE

13. ABSTRACT (*Maximum 200 words*)

MPD thrusters have demonstrated between 2000 and 7000 seconds specific impulse at efficiencies approaching 40%, and have been operated continuously at power levels over 500 kW. These demonstrated capabilities, combined with the simplicity and robustness of the thruster, make them attractive candidates for application to both unmanned and manned orbit raising, lunar, and planetary missions. To date, however, only a limited number of thruster configurations, propellants, and operating conditions have been studied. This work reviews the present status of MPD thruster research, including developments in the measured performance levels and electrode erosion rates, and theoretical studies of the thruster dynamics. Significant progress has been made in establishing empirical scaling laws, performance and lifetime limitations and in the development of numerical codes to simulate the flow field and electrode processes.

14. SUBJECT TERMS	15. NUMBER OF PAGES
Electric propulsion; Space propulsion; Nuclear electric propulsion	34
	16. PRICE CODE A03

17. SECURITY CLASSIFICATION OF REPORT	18. SECURITY CLASSIFICATION OF THIS PAGE	19. SECURITY CLASSIFICATION OF ABSTRACT	20. LIMITATION OF ABSTRACT
Unclassified	Unclassified	Unclassified	